Impacts of future land use and land cover change on mid-21st-century surface ozone air quality: Distinguishing between the biogeophysical and biogeochemical effects

Lang Wang[1,2], Amos P. K. Tai[1,3,4], Chi-Yung Tam[1,3], Mehliyar Sadiq[1,3], Peng Wang[3], Kevin K. W. Cheung[5]

1 Institute of Environment, Energy and Sustainability, The Chinese University of Hong Kong, Hong Kong, China

2 Department of Geography and Resource Management, The Chinese University of Hong Kong, Hong Kong, China

3 Earth System Science Programme, Faculty of Science, The Chinese University of Hong Kong, Hong Kong, China

4 Partner State Key Laboratory of Agrobiotechnology, The Chinese University of Hong Kong, Hong Kong, China

5 Department of Environmental Sciences, Macquarie University, Sydney, Australia

Prepared for Atmospheric Chemistry and Physics

September 2019

Abstract

Surface ozone (O_3) is an important air pollutant and greenhouse gas. Land use and land cover is one of the critical factors influencing ozone, in addition to anthropogenic emissions and climate. Land use and land cover change (LULCC) can on the one hand affect ozone “biogeochemically”, i.e., via dry deposition and biogenic emissions of volatile organic compounds (VOCs). LULCC can on the other hand alter regional- to large-scale climate through modifying albedo and evapotranspiration, which can lead to changes in surface temperature, hydrometeorology and atmospheric circulation that can ultimately impact ozone “biogeophysically” over local and remote areas. Such biogeophysical effects of LULCC on ozone are largely understudied. This study investigates the individual and combined biogeophysical and biogeochemical effects of LULCC on ozone, and explicitly examines the critical pathway for how LULCC impacts ozone pollution. A global coupled atmosphere-chemistry-land model is driven by projected LULCC from the present day (2000) to future (2050) under RCP4.5 and RCP8.5 scenarios, focusing on the boreal summer. Results reveal that when considering biogeochemical effects only, surface ozone is predicted to have slight changes by up to 2 ppbv maximum in some areas due to LULCC. It is primarily driven by changes in isoprene emission and dry deposition counteracting each other in shaping ozone. In contrast, when considering the integrated effect of LULCC, ozone is more substantially altered by up to 6 ppbv over several regions, reflecting the importance of biogeophysical effects on ozone changes. Furthermore, large areas of these ozone changes are found over the regions without LULCC where the biogeophysical effect is the only pathway for such changes. The mechanism is likely that LULCC induces a regional circulation response, in particular the formation of anomalous stationary high-pressure systems,

shifting of moisture transport, and near-surface warming over the middle-to-high northern latitudes in boreal summer, owing to associated changes in albedo and surface energy budget. Such temperature changes then alter ozone substantially. We conclude that the biogeophysical effect of LULCC is an important pathway for the influence of LULCC on ozone air quality over both local and remote regions, even in locations without significant LULCC. Overlooking the impact of biogeophysical effect may cause evident underestimation of the impacts of LULCC on ozone pollution.

Keywords: ozone pollution; land use and land cover change; biogeochemical effects; biogeophysical effects

1. Introduction

Surface ozone (O_3), as a harmful air pollutant, has negative consequences for human health (WHO, 2005; Jerrett et al., 2009; Malley et al., 2017), decreases plant gross primary productivity (e.g., Yue and Unger 2014), and leads to substantial reductions in global crop yields (Avnery et al., 2011; Tai et al., 2014; Tian et al., 2016; Tai and Val Martin, 2017; Mills et al., 2018). It is also an important greenhouse gas, contributing to climate change (Myhre et al., 2013). Surface ozone is produced by the photooxidation of precursors including carbon monoxide (CO), methane (CH_4), and other non-methane volatile organic compounds (NMVOCs) in the presence of nitrogen oxides (NO_x). These precursors are both generated by human activities and naturally emitted from vegetation and soils. The dominant sink of surface ozone is photochemical loss and dry deposition to the surface including vegetation mainly in the form of leaf stomatal uptake. Depending on all of these production and loss mechanisms, its concentration is highly sensitive to changes in natural and anthropogenic emissions of precursors (Wang et al., 2011), land use and land cover (Ganzeveld et al., 2010; Val Martin et al., 2015; Fu and Tai, 2015) and climate (Jacob and Winner, 2009; Fiore et al., 2012; Schnell et al., 2016). Recent studies found that decreases in anthropogenic emissions alone might not necessarily decrease ozone in some polluted regions if factors such as climatic and land cover changes act to enhance ozone and offset emission control efforts (Zhou et al., 2013; Zhang et al., 2014; Xue et al., 2014).

Land use and land cover change (LULCC) can modify ozone concentration by altering key drivers of ozone such as biogenic VOC emissions and dry deposition (e.g., Wong et al., 2018). These can be referred to as “biogeochemical effects” of LULCC on ozone (as opposed to “biogeophysical effects”, which will be discussed

next), because these processes entail directly modifying the biosphere-atmosphere exchange of gases and particles that alters atmospheric composition including ozone itself. Here we limit the "biogeochemical effects" of LULCC on ozone to processes that influence ozone directly in a given climate, including biogenic VOC emission and the dry deposition of ozone and its precursors; climatic changes that can arise from land cover disturbances of the biogeochemical cycles are not the focus.

LULCC can modify the spatial pattern and magnitude of isoprene emission due to their strong dependence on vegetation type and leaf density (Guenther et al., 2012). For instance, Lathière et al. (2006) found as much as a 29% decrease in global isoprene emission from a scenario in which 50% tropical trees are replaced by grasses. Heald and Spracklen (2015) estimated the net effect of LULCC under future anthropogenic influences as a decrease of 12–15% in annual isoprene emission globally. These changes in isoprene emission can in turn modify ozone concentration. For example, Tai et al. (2013) found that LULCC projections in the Intergovernmental Panel on Climate Change (IPCC) A1B scenario with widespread crop expansion could reduce isoprene emission by ~10% globally compared with the land use and land cover at present. Such a reduction could correspondingly lead to an up to 4 ppbv of ozone decrease in the eastern US and western Europe, and an up to 6 ppbv increase in South and Southeast Asia, whereby the difference in the sign of responses is driven primarily by the different ozone production regimes.

Dry deposition is another key factor modulating ozone (e.g., Wesely, 1989; Val Martin et al., 2014; Lin et al., 2019). Dry deposition is the most efficient over densely vegetated regions via the stomatal uptake of ozone and its precursors, and LULCC can alter these fluxes. Kroeger et al. (2013) found that reforestation over peri-urban areas in Texas, USA, could effectively enhance dry deposition, resulting in

decreases in ozone and its precursors. Fu and Tai (2015) found that LULCC driven by climate and CO_2 changes could overall enhance dry deposition and decrease ozone by up to 4 ppbv in East Asia during the past three decades. The dry deposition enhancement mostly arises from climate- and CO_2-induced increase in leaf area index (LAI), which more than offsets the compensating effect of cropland expansion (Fu and Tai, 2015). The relative importance of isoprene emission and dry deposition, which could have counteracting effects on ozone given the same LULCC, is strongly dependent on local NO_x concentrations and vegetation type (Wong et al., 2018).

LULCC can also affect weather and climate over local and remote regions by perturbing the biosphere-atmosphere exchange of water and energy fluxes (e.g., Betts, 2001; Bonan, 2016; Pitman et al., 2009). For example, afforestation generally cools the surface in tropical regions, where evaporative cooling generally exceeds radiative warming from reduced albedo, but warms the surface in boreal forests due to the more dominant radiative warming effect (e.g., Arora and Montenegro, 2011; Lee et al., 2011; Bonan, 2008). There is little consensus on the effects of afforestation in midlatitude regions (e.g., Boisier et al., 2012; de Noblet-Ducoudré et al., 2012). Furthermore, the impacts of such surface forcing could extend into the upper troposphere, alter large-scale circulation pattern, and consequently affect the climate in remote regions (Henderson-Sellers et al. 1993; Chase et al., 2000; Swann et al., 2012). Recent studies (Devaraju et al. 2015; Laguë and Swann 2016) have identified that LULCC in midlatitude regions can modify the global energy balance, impacting cloud cover, precipitation, and circulation pattern via remote effects. By and large, the impacts of LULCC on the atmosphere is complex. Laguë et al. (2019) examined the climatic effects of individual physical components in the land surface (albedo, evaporative resistance and surface roughness), and found that temperature responds

most to changes in albedo and evaporative resistance, particularly in the extra-tropics through large-scale atmospheric feedbacks. Still, how individual land characteristics play out together and interact with each other to affect the atmospheric general circulation, and how the surface signals may translate into those in the upper levels are not fully understood.

Such a modification of the overlying meteorological environment and climate induced by LULCC and the associated exchange of momentum, heat and moisture between the land and atmosphere can be defined as "biogeophysical effects" of LULCC. Such effects can further alter surface ozone on local to pan-regional scales (Jiang et al., 2008; Ganzeveld et al., 2010; Wu et al., 2012), and we shall call these and related pathways the biogeophysical effects of LULCC on ozone. In particular, a LULCC-induced increase in surface temperature could (1) accelerate peroxyacetyl nitrate (PAN) decomposition into NO_x (Jacob and Winner, 2009; Doherty et al., 2013; Pusede et al., 2015), (2) increase biogenic VOCs emissions from vegetation (Guenther et al., 2012; Wang et al., 2013; Squire et al., 2014), and (3) lead to more water vapor in air that tends to increase ozone destruction (Jacob and Winner, 2009) (Fig. 1). The net effect of higher temperatures is almost always ubiquitously an enhancement of ozone levels reported from both observational (e.g., Porter et al., 2015; Pusede et al., 2015) and modeling (e.g., Shen et al., 2016; Lin et al., 2017) studies in many polluted regions.

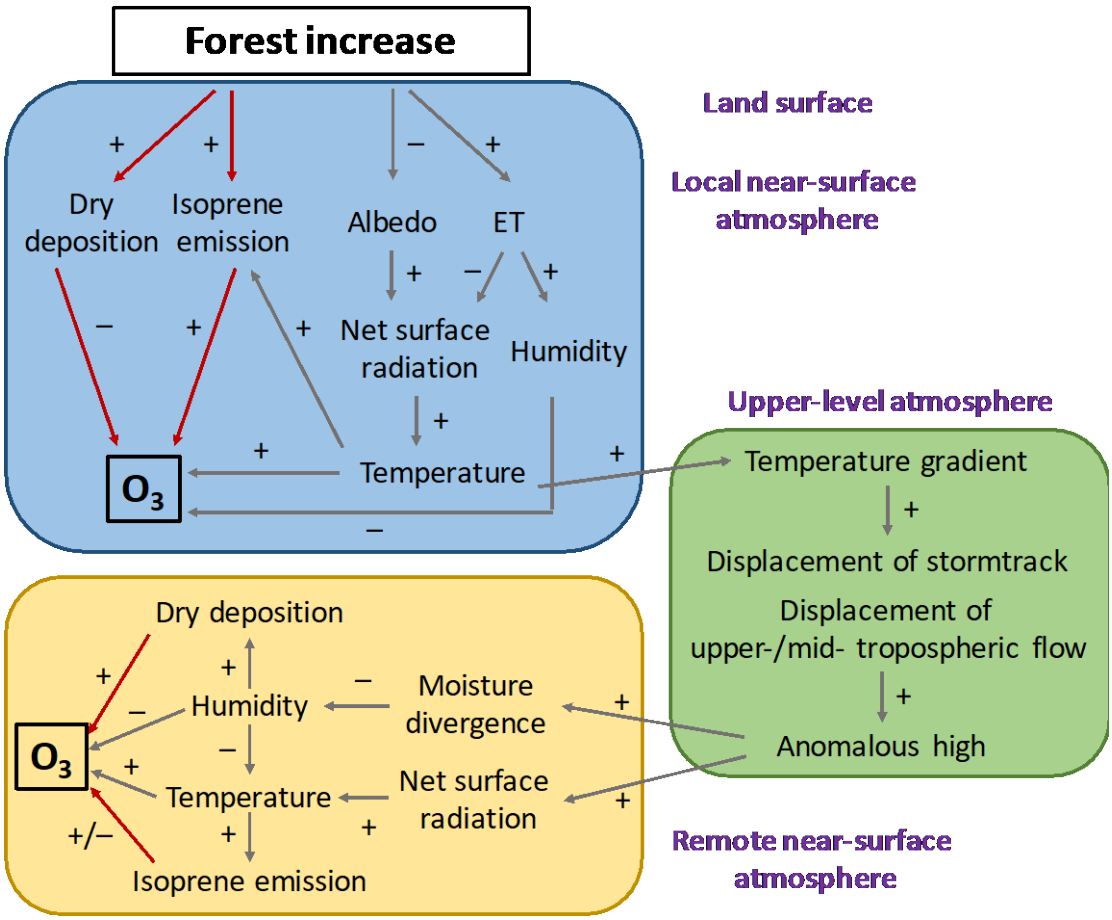

Figure 1. Schematic diagram showing the biogeochemical and biogeophysical effects of land use and land cover change (LULCC) on surface ozone, using a case where forest coverage increases (e.g., under the RCP4.5 scenario) as an example. Red arrows indicate biogeochemical effects and grey arrows indicate biogeophysical effects. We focus on processes initiated at the land surface by LULCC, and the corresponding responses in local near-surface atmosphere (blue box), middle- to upper-level atmosphere (green box) and remote near-surface atmosphere (yellow box).

The LULCC biogeophysical effects have thus far been largely unexplored, though biogeochemical effects of LULCC have been examined by a number of studies (Wu et al., 2012; Fu and Tai, 2015; Heald and Geddes, 2016). Only a few recent studies have implicitly included such biogeophysical effects of LULCC in their coupled land-atmosphere models when assessing the impacts of LULCC on surface ozone. Val Martin et al (2015) studied the integrated effects of LULCC on surface

ozone using future LULCC scenarios, and found an increase of 2–3 ppbv from 2000 to 2050 over US national parks. Ganzeveld et al. (2010) also calculated the future LULCC from 2000 to 2050, and found that an increase in boundary-layer ozone mixing ratios by up to 20% over the tropics. However, these studies did not distinguish between the roles of biogeophysical vs. biogeochemical effects, or decipher the physics and relative importance of various mechanisms behind the integrated effects.

The aim of this study is to investigate how and to what extent global LULCC could affect surface ozone in the near future by investigating and distinguishing between the biogeochemical, biogeophysical and integrated effects of LULCC. We suggest a new line of biogeophysical pathways linking LULCC to surface ozone, and also consider biogeochemical pathways through isoprene emission and dry deposition changes caused by LULCC. In particular, over the regions without significant LULCC but showing substantial ozone changes, we find that the biogeophysical effects arising from LULCC-induced atmospheric circulation changes can be dominant and could be isolated from the integrated effects. LULCC is one of the key strategies for climate change mitigation, but meanwhile has substantial impacts on ozone pollution. Understanding its comprehensive pathways on surface ozone can help provide important references for integrated air quality and land use management in the future.

2. Data and methods

2.1 Modeling framework

To simulate the impacts of LULCC on surface ozone, we use the Community Earth System Model (CESM) version 1.2 (http://www.cesm.ucar.edu/models/), which is a comprehensive global model that couples different independent components for

197 the atmosphere, land, ocean, sea ice, land ice and river runoff (Lamarque et al., 2012).
198 The atmospheric component is the Community Atmosphere Model version 4
199 (CAM4), which uses a finite-volume dynamical core with comprehensive
200 tropospheric and stratospheric chemistry (CAM-Chem). Chemical mechanisms are
201 based on the Model for Ozone and Related chemical Tracers (MOZART) version 4
202 (Emmons et al., 2010). For the land component, the Community Land Model (CLM)
203 version 4.5 (Oleson, 2013) considers 16 Plant Function types (PFTs) (Lawrence et al.,
204 2011), and prescribes the total leaf area index (LAI), the PFT distribution and PFT-
205 specific seasonal LAI derived from Moderate Resolution Imaging Spectroradiometer
206 (MODIS) observations. We use the Satellite Phenology (SP) mode of CLM4.5 for all
207 simulations, which prescribes vegetation structural variables including LAI and
208 canopy height; active biogeochemical cycling in terrestrial ecosystems is not turned
209 on.

210 In CLM4.5, biogenic VOC emissions are computed using the Model of
211 Emissions of Gases and Aerosols from Nature (MEGAN) version 2.1 (Guenther et al.,
212 2012), accounting for the major known processes controlling biogenic VOC
213 emissions from terrestrial ecosystems, such as effects of temperature, solar radiation,
214 soil moisture, leaf age, CO_2 concentrations, and vegetation species and density.
215 Biogenic VOC emissions in MEGAN are allowed to respond interactively to changes
216 of these processes. Thus, isoprene emission is allowed to respond to spatiotemporal
217 changes in PFTs and the associated changes in meteorological conditions in this
218 study. Dry deposition of gases and aerosols are computed based on the multiple
219 resistance approach of Wesely (1989), updated by Emmons et al. (2010), Lamarque et
220 al. (2012) and Val Martin et al. (2014). In the scheme, dry deposition velocity is the
221 inverse of aerodynamic resistance (R_a), sublayer resistance (R_b) and bulk surface

resistance (R_c), whereby R_c includes a combination of resistances from vegetation (including stomatal resistance), lower canopy, and ground with specific values for different land types. Correspondingly, dry deposition velocity in the scheme responds to primarily meteorological and ecophysiological conditions. Soil NO_x emissions are dependent on soil moisture, soil temperature and vegetation cover (Emmons et al., 2010; Yienger and Levy, 1995), while biomass burning emissions and anthropogenic emissions of ozone precursors, are prescribed by inventory at present-day levels.

The coupled CAM-Chem-CLM model configuration of CESM can be run with prescribed meteorology to drive atmospheric chemistry-only simulations (hereafter as dynamical Off-line mode), or with interactive, dynamically simulated meteorology using CAM4 (hereafter as On-line mode). These two modes are both applied in the study. In particular, the Off-line mode is used to quantify the biogeochemical effects of LULCC alone on surface ozone in the absence of any associated meteorological responses to LULCC. The On-line mode is applied to assess the biogeophysical and integrated effects on ozone caused by LULCC, considering also the effects of the resulting meteorological changes.

For the Off-line mode, we use the Goddard Earth Observing System Model Version 5 (GEOS-5) (https://rda.ucar.edu/datasets/ds313.0/) (Tilmes, 2016) assimilated meteorology as the driving fields, with a horizontal resolution of 1.9°×2.5° and 56 vertical levels between the surface and the 4-hPa level. For the On-line mode of CAM4-Chem-CLM, 26 vertical levels are used between the surface and 4 hPa, with the same horizontal resolution as the Off-line mode. For all simulations, concentrations of long-lived greenhouse gases including CO_2, CH_4, and N_2O are prescribed at present-day. For the anthropogenic emissions used for all simulation are described in Lamarque et al. (2010, 2012) and references therein. Climatic changes

247 that may arise from land cover disturbances of the terrestrial carbon and nitrogen
248 cycles are not the focus of this study, which aims to delineate the more immediate
249 responses of surface ozone to LULCC.

250 The CAM-Chem-simulated atmospheric chemistry has been extensively
251 evaluated and documented (e.g., Lamarque et al., 2012). In general, CAM-Chem can
252 reasonably replicate observed values at individual sites (CASTNET for US and
253 EMEP for Europe) (Lamarque et al., 2012; Val Martin et al., 2014; Sadiq et al.,
254 2017), mid- and upper-tropospheric observations (Lamarque et al., 2010) albeit with a
255 general overestimation; and the performance is comparable to other global and
256 regional models (Lapina et al., 2014; Parrish et al., 2014). Uncertain emissions, coarse
257 resolution (Lamarque et al., 2012), misrepresentation of dry deposition process (Val
258 Martin et al., 2014) and overestimation of stomatal resistance (Lin et al., 2019) are all
259 likely factors contributing to these high biases.

260 *2.2 Present and future land use and land cover scenarios*

261 For the present-day land cover distribution, satellite phenology based on
262 MODIS and a cropping dataset from Ramankutty et al. (2008) are used (see Lawrence
263 et al., 2011). The cropping dataset combines agricultural inventory data and two
264 satellite-derived land products. For the future land cover, projections based on the
265 Representative Concentration Pathways (RCP) 4.5 and 8.5 scenarios are adopted (van
266 Vuuren et al., 2011). Both are computed using Integrated Assessment Models (IAM)
267 for the Phase 5 of the Coupled Model Intercomparison Project (CMIP5) community,
268 incorporating anthropogenic transformation and activities associated with carbon
269 releases (e.g., wood harvest). These LULCC projections are internally consistent with
270 the corresponding emission scenarios and development pathways for the Fifth
271 Assessment Report (AR5) of Intergovernmental Panel on Climate Change (IPCC)

(Taylor et al., 2012). In general, the RCP4.5 LULCC has the most extensive use of land management as a carbon mitigation strategy, with the expansion of forest areas combined with large reductions in croplands and grasslands. The RCP8.5 LULCC has the least effective use of land management for carbon mitigation, with large expansion in both croplands and grasslands together with substantial forest losses. In this study, emissions are held constant at the present-day level for all runs, thus the effects of LULCC can be considered as being decoupled from changes in anthropogenic emissions in order to isolate the effects of LULCC alone.

Both present-day and future land cover are transformed into PFTs changes for implementation into CESM (Lawrence et al., 2012; Oleson et al., 2013). The long-term time series of LULCC span through the historical (1850–2005) and future (2006–2100) periods in 5-year intervals (Riahi et al., 2007; van Vuuren et al., 2007; Wise et al., 2009a), and are then interpolated and harmonized with smooth transitions on the annual timescale (Hurtt et al., 2011). For this work, we focus on LULCC from the present-day (2000) to future (2050) period.

2.3 Model experiments

We have two sets of configuration, Off-line mode and On-line mode, with eight simulations to investigate the impacts of LULCC on surface ozone (see Table 1). We focus on boreal summer month (June-July-August, JJA) averages as this is the period when ozone pollution is generally the most severe in the Northern Hemisphere (NH). In the first set of simulations in Off-line mode, surface ozone would respond to LULCC only through biogeochemical effects that mainly include changes in dry deposition velocity and isoprene emissions due to different LULCC scenarios without meteorological responses to LULCC. The Off-line mode includes control run (Off-line_CTL) using present-day (year 2000) distribution of land use and land cover, and

two future simulations Off-line_45 and Off-line_85, with year-2050 land use and land cover distribution following RCP4.5 and RCP8.5, respectively. All three experiments are time-sliced simulations using prescribed GEOS-5 meteorology from 2004 to 2017 for 14 years allowing for interannual climate variability, and we use the last 10-year averages for analysis. The statistical significance of the comparison amongst these experiments was assessed by the Student's t-test at the 90% confidence levels.

304

	Case Name	Land forcing	Meteorolog	Simulated years	Other settings
1	Off-line_CTL	Present-day (2000) land use and land cover map	GEOS-5 reanalysis (2004-2017)	14 years The last 10 years average for analysis	- Present-day (2000) well-mixed greenhouse gases and short-lived gases and aerosols, anthropogenic emissions; - Present-day (2000) monthly mean sea surface temperature and sea ice -All simulations use the SP mode in CLM - Isoprene emission is from MEGAN - Dry deposition velocity is based on Wesely (1989) updated by Val Martin et al. (2014)
2	Off-line_45	2050 RCP4.5 scenario future land use and land cover map in time slice	GEOS-5 reanalysis (2004-2017)	14 years The last 10 years average for analysis	
3	Off-line_85	2050 RCP8.5 scenario future land use and land cover map in time slice	GEOS-5 reanalysis (2004-2017)	14 years The last 10 years average for analysis	
4	On-line_CTL	Present-day (2000) land use and land cover map	Simulated online	55 years The last 10 years average for analysis	
5	On-line_45	2000-2005 historical, 2006-2059 RCP4.5 scenario transient land use and land cover map	Simulated online	55 years The last 10 years average for analysis	
6	On-line_85	2000-2005 historical, 2006-2059 RCP8.5 scenario transient land use and land cover map	Simulated online	55 years The last 10 years average for analysis	
7	On-line_45TS	2050 RCP4.5 scenario future land use and land cover map in time slice	Simulated online	55 years The last 10 years average for analysis	
8	On-line_85TS	2050 RCP8.5 scenario future land use and land cover map in time slice	Simulated online	55 years The last 10 years average for analysis	

305

306 Table 1. List of model experiments. There is one ensemble member considered for each “On-line” model
307 simulation; for Cases 4, 7 and 8, since the same annual forcings are used for 55 years of simulation, each year of
308 simulation can be treated as one of the 55 pseudo-ensemble members.

In the second set of five On-line mode simulations, ozone would respond to both the biogeochemical and biogeophysical effects caused by future projected LULCC and LULCC-induced meteorological changes. The first experiment On-line_CTL, reflects present-day conditions and uses land surface forcing for year 2000. The second and third experiments, referred to as On-line_45 and On-line_85, are transient simulations performed continuously from year 2000 to 2059 using transient land cover maps projected for the RCP4.5 and RCP8.5 scenarios, respectively. The fourth and fifth experiments, On-line_45TS and On-line_85TS, are time-sliced simulations using 2050 land cover distribution following RCP4.5 and RCP8.5, respectively. These two experiments are designed for paralleled comparison with Off-line mode simulations, and for additional comparison between the impacts of LULCC using time-sliced runs and transient runs on ozone pollution and related pathways in the model. All five On-line experiments are run for 55 years, and the last ten years are used for analysis after modeled variables have attained a quasi-steady state. Our experiments all start from an equilibrium (spun-up) state for the year 2000; the spun-up state uses offline CLM run for 50 years forced by the cycling year 2000 of the Qian et al. (2006) atmospheric conditions. All simulations are performed with prescribed sea surface temperature and sea-ice cover following the HadISST data set (Rayner et al., 2003) at the year-2000 level. Long-lived greenhouse gases and thus the radiative forcing from them are kept at present-day conditions (year 2000) to isolate the effects of LULCC only.

These eight sets of model configuration allow us to separate and examine: (1) biogeochemical effects of LULCC on surface ozone, (2) biogeophysical effects on surface ozone, and (3) the integrated effects induced by LULCC on surface ozone and its precursors and dry deposition.

3. Results

3.1 Projected land use and land cover change from 2000 to 2050

Fig. 2 shows the global distribution of present-day (year 2000) PFTs and future projected changes (2000 to 2050) following RCP4.5 and RCP8.5 for three major land cover categories. The future LULCC in RCP4.5 is characterized by extensive forest expansion (Figs. 2f, g). Transition from present-day to 2050 in RCP4.5 highlights the global growth of forest from 71.8 million to 74.0 million km^2, at the expense of croplands (from 14.7 million to 12.3 million km^2); grasslands slightly increase in area from 33.7 million to 33.8 million km^2. The net increase of 2.2 million km^2 of forests is consistent with that provided by Hurtt et al. (2011), Lawrence et al. (2012) and Heald and Geddes (2016). Fig. 2f also illustrates cropland area increases over Southeast Asia, India and China. Such increases are due to more bioenergy crop production for the purpose of climate change mitigation, economic advantages from agriculture productivity growth, lower regional land prices, and availability of undeveloped lands in these developing regions (Wise et al., 2009b; Thomson et al., 2011). In contrast, regions such as Europe, US and Canada, undergo extensive reforestation. RCP8.5 LULCC is characterized by extensive cropland expansion (Figs. 2k, l, m), driven mainly by a large increase in the global population and a slow increase in crop yields due to a slow rate of exchange of technology globally (Riahi et al., 2011). Cropland expansion occurs largely over the tropical belt (30°N-30°S) at the expense of forest reduction. The total increases in croplands are by 1.8 million km^2, and forest area decreases by 2.5 million km^2.

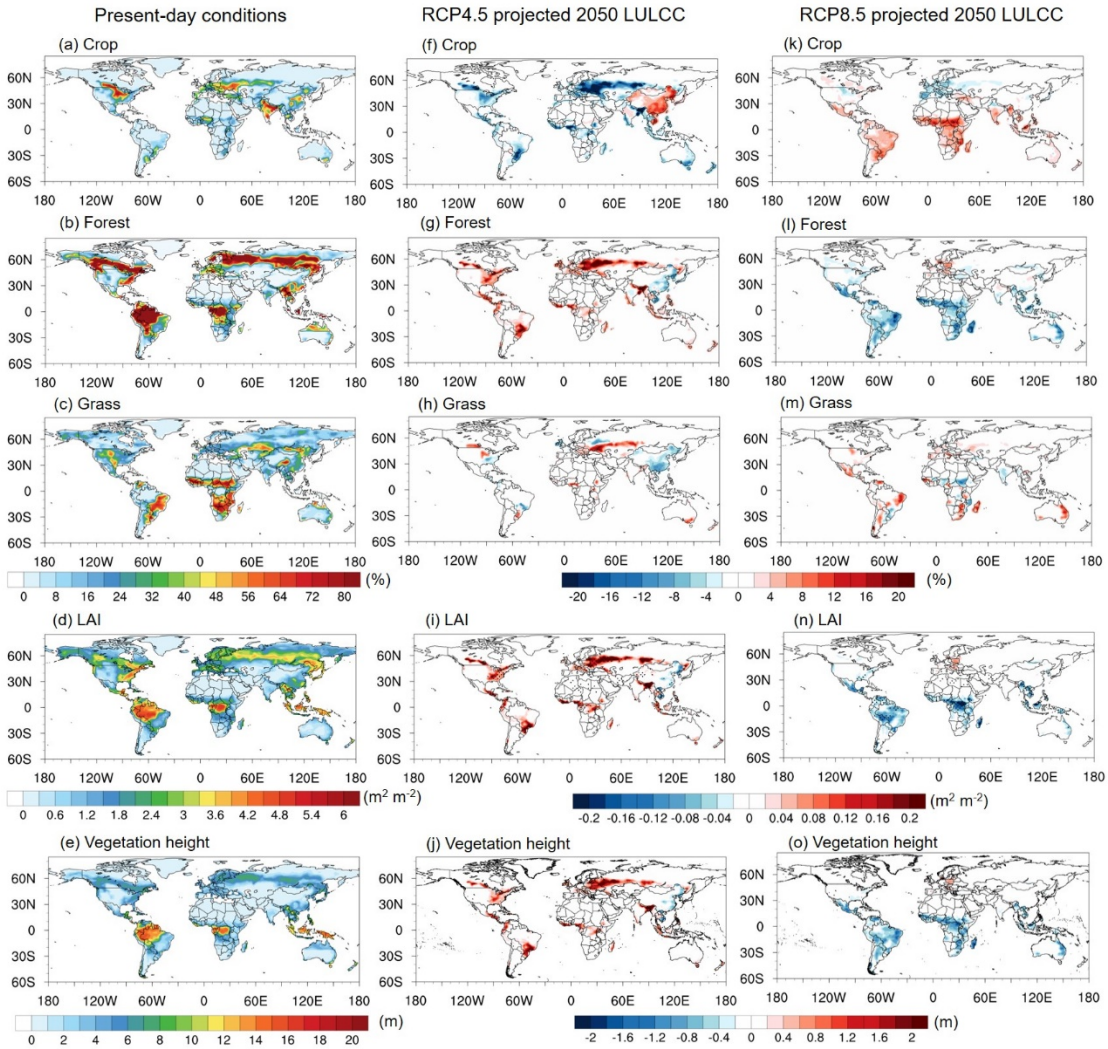

Figure 2. Present-day (2000) land use and land cover by percentage of land coverage, total leaf area index (LAI) and vegetation height (left), and their changes from 2000 to 2050 under RCP4.5 (middle) and RCP8.5 (right) scenarios for the boreal summer (June-July-August) (units at the right side of the color bar). Plant function types (PFTs) in CESM are here grouped into three major categories: crop, forest and grass. The treatment of vegetation including PFT fractional coverage, LAI and canopy height is prescribed using the SP mode of CLM4.5 in both the present-day case and future LULCC scenarios. For the future cases, PFT fractional coverage is derived according to the RCP land use scenarios.

The present-day LAI and its changes associated with the future projected LULCC are shown in Figs. 2d, 2i and 2n. Forest expansion leads to increases in LAI, whereas deforestation results in LAI reduction. For RCP4.5, due to the widespread

reforestation and afforestation except in East Asia, LAI increases significantly. Particularly over Europe and the US, the absolute increase in LAI is > 0.1. For RCP8.5, LAI generally declines with intense reductions over the tropical regions.

3.2 Biogeochemical effects of land use and land cover change on surface ozone

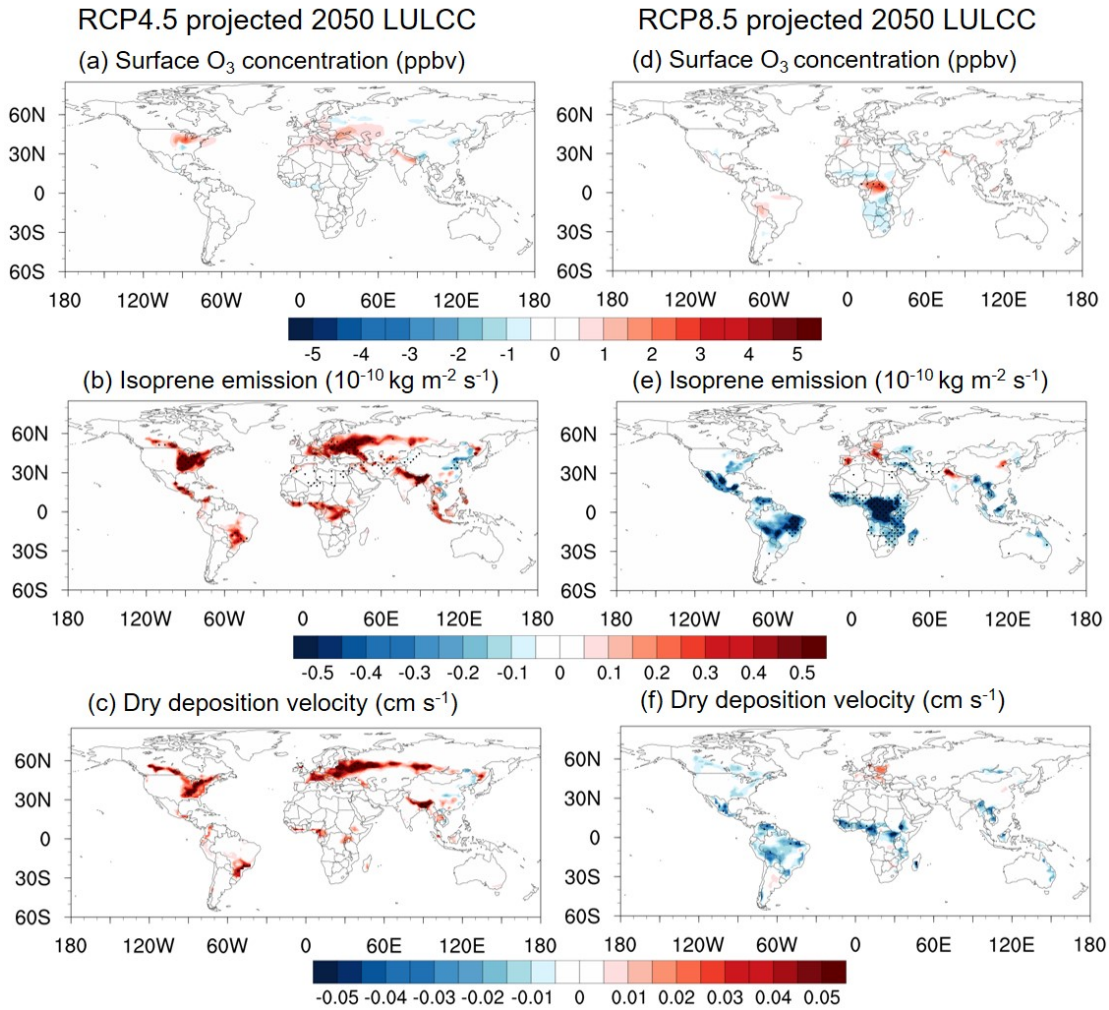

Figure 3. Simulated 2000-to-2050 changes in surface ozone, isoprene emission, and dry deposition velocity under RCP4.5 and RCP8.5 projected LULCC for the boreal summer (June-July-August) averaged for the final 10 years of simulations. Regions with dots indicate changes that are significant at the 90% confidence level. These are results from Off-line runs with prescribed meteorology; i.e., meteorological variables do not respond to LULCC.

Using the Off-line configuration, we find that isoprene emission changes correspond closely with the LULCC in each future scenario from 2000 to 2050 (Figs.

382 3b, e). For RCP4.5, isoprene emission increases over the regions with forest
383 expansion, including the US, Europe and some tropical regions, but decreases over
384 East Asia. Such isoprene emission increases are primarily driven by forest expansion,
385 since forest PFTs typically emit much more isoprene than crops and grasses
386 (Guenther et al., 2012). For RCP8.5, isoprene emission decreases over the tropics
387 with slight increases over Europe, north China and north India, largely due to forest
388 reduction in this scenario.

389 Table 2 summarizes the percentage and absolute changes of the annual global
390 isoprene emission. The simulated present-day annual global isoprene is 353.8 Tg C
391 yr^{-1}, in the middle of the range 308–678 Tg C yr^{-1} summarized by Guenther et al.
392 (2012). For the RCP4.5 LULCC, the annual global isoprene emission increases by
393 5.2%, but it decreases by 11.8% for RCP8.5. The isoprene emission changes are in
394 line with these studies by Heald et al. (2008) and Wu et al. (2012), who estimated a
395 decrease of 12–15% in global isoprene emission under the net biogeochemical effect
396 of future LULCC (A1B and A2 scenarios).
397

398

		Isoprene emissions (TgC yr^{-1})	% change	Ozone dry depositional sink (Tg yr^{-1})	% change	Ozone concentration (ppbv)	% change
Off-line	Off-line_CTL	353.8		886.8		23.6	
	Off-line_45	372.3	5.2	895.4	1.0	23.7	0.4
	Off-line_85	311.9	–11.8	879.8	–0.8	23.5	–0.4
On-line	On-line_CTL	419.4		969.7		25.6	
	On-line_45	433.6	3.4	973.3	0.4	25.9	1.2
	On-line_85	386.1	–7.9	964.7	–0.5	25.8	0.8
	On-line_45TS	434.6	3.6	975.9	0.6	25.9	1.2
	On-line_85TS	383.8	–8.5	961.7	–0.8	25.7	0.4

399

400 Table 2. Summertime average (June-July-August) global isoprene emission and ozone dry-depositional sink as
401 influenced by future LULCC in the RCP4.5 and RCP8.5 scenarios; shown separately are changes in prescribed
402 meteorology (biogeochemical effects only) and coupled atmosphere-chemistry-land configurations (both
403 biogeochemical and biogeophysical effects).

Fig. 3c shows that LULCC in the RCP4.5 scenario has enhanced dry deposition velocity over most regions where forests have expanded. Forest with both large LAI, and high surface roughness often provides the highest dry deposition velocity amongst all PFTs (Emmons et al., 2010; Lamarque et al., 2012). The most dramatic changes occur in Europe where local maximum changes occur in land cover between forests and croplands. Local decreases over East Asia are the result of deforestation. For RCP8.5, dry deposition velocity decreases mostly over the regions where tropical forests are replaced by croplands (Fig. 3f). Equatorial Africa and the Amazon experience the largest decrease in dry deposition velocity relative to present-day conditions. Some increases over Western Europe are the result of local reforestation.

The globally averaged change in the dry-depositional sink is around 1% (Table 2). Local dry deposition velocity changes within 0.05 cm s^{-1}. The value of dry deposition velocity change is in line with previous studies exploring future 2050 LULCC alone on the dry deposition velocity of ozone (e.g., Verbeke et al., 2015), though our results show slightly larger changes due to larger LAI differences between forests and crops/grasses during the boreal summer compared with their annual mean values of differences from Verbeke et al. (2015).

Figs. 3a and 3d show the impacts of future projected LULCC on surface ozone. LULCC under RCP4.5 with massive forest expansion increases isoprene emission that could increase surface ozone, but also enhance dry deposition velocity that could reduce surface ozone. The overall changes in surface ozone are thus generally small due to these compensating effects. There are a few regions with surface ozone changes by up to 2 ppbv. In particular, over the US, opposite surface ozone changes are seen in RCP4.5: an increase in the northeast US and a decrease in

the southeast US despite of the fact that both changes are driven by forest expansion (Fig. 3a). Such a contrasting pattern is shaped by the local atmospheric chemical conditions related to O_3-NO_x-VOC chemistry. The northeast US is a high-NO_x region, and increases in isoprene emission result in enhanced ozone, more than offsetting the effect of increasing dry deposition velocity. In contrast, the southeast US is a high-isoprene-emitting region; additional isoprene may react with ozone and NO_x, thereby suppressing surface ozone production (Kang et al., 2003; von Kuhlmann et al., 2004; Fiore et al., 2005; Pfister et al., 2008). Furthermore, in the low-NO_x region, OH is largely removed by reactions with biogenic VOCs, producing peroxy radicals that form HO_2 or producing organic peroxides. Recent studies found that organic peroxide formation can be reduced; alternatively, these peroxides could be rapidly photolyzed, making them at best a temporary HO_x reservoir (e.g., Thornton et al., 2002; Kubistin et al., 2010). This result implies that in low-NO_x regions ozone production may be NO_x-saturated more often than current models suggest. Suppressed ozone is also found in the tropical regions of South America and Africa (Fig. S1a). Together with the increase in dry deposition velocity, overall there is a decrease of surface ozone. Similar to the northeastern US conditions, southern Europe, northeastern India and northern China are also high-NO_x regions.

Under the RCP8.5 scenario with substantial cropland and grassland expansion, decrease in isoprene emission and dry deposition again offset each other in controlling surface ozone in high-NO_x regions. Surface ozone concentration decreases by around 1 ppbv over the north-central and southern Africa, but increases by up to 2 ppbv over equatorial Africa and central South America (Fig. 3d). In particular, the area with enhanced ozone in these regions corresponds well with reductions in isoprene emission and dry deposition together. Equatorial Africa is a high-isoprene-

emitting, low-NO_x region, thus decreases of isoprene emission together with reduced dry deposition would lead to enhanced ozone (Fig. S1b).

3.3 Biogeophysical effects of land use and land cover change on surface ozone

Next, we examine results from the On-line simulations, which allow us to assess the impacts of LULCC on surface ozone when the overlying meteorological environment is also modified by LULCC. The simulated changes in surface ozone is in the range from –3 to +6 ppbv (Figs. 4a, e). The magnitude of ozone changes in On-line simulations is overall larger than those in Off-line simulations (Table 2), which consider biogeochemical effects only, indicating the importance of complications from the changing meteorological environment in response to LULCC. Within the On-line simulations, more substantial responses of temperature as well as of surface ozone to LULCC are found in RCP4.5 compared with those in RCP8.5.

In contrast to the clear, localized signals in ozone changes in response to LULCC through biogeochemical pathways, surface ozone changes are more complex when biogeophysical pathways are also involved (Figs. 4a, e). Most importantly, both local and remote ozone changes can be discerned. In particular, ozone changes, together with changes in isoprene emission (Figs. 4b, f) and dry deposition (Figs. 4c, g) are found in regions without much LULCC. Such signals are not captured by the Off-line simulations in which changes only respond to LULCC locally (Fig. 3). On the other hand, changes in surface temperature are found to be correlated well with patterns of changes in ozone (Fig. S2a, d), indicating that the biogeophysical drivers that modify temperature may play critical roles in ozone changes. In the regions where temperature increases, surface ozone increases correspondingly. Figs. 4d and 4h show simulated changes in near-surface air temperature (below the 850 hPa level) from 2000 to 2050. Regional-scale temperature changes of up to 2 K are found. Such

magnitudes of temperature anomalies induced by LULCC are in line with those from previous experiments (Lawrence et al., 2012; Brovkin et al., 2013). Both local and remote temperature changes could be driven by LULCC. Over the regions where temperature increases, surface ozone increases correspondingly.

Changes in isoprene emission also correlate with temperature changes (Figs. 4b, d; Figs. 4f, h, Fig. S2b). Isoprene emission also increases in regions with forest expansion, reflecting not only the biogeochemical effects due to higher fractional coverage of isoprene-emitting vegetation types (Section 3.2), but also the biogeophysical effects arising from changing land surface temperature.

Changes in dry deposition velocity (Figs. 4c, g, Fig. S2c) also correlate to meteorological changes. In the dry deposition scheme, stomatal resistance can respond to atmospheric dryness and soil water stress. For instance, drier conditions are captured in RCP4.5 in the central-western US as initiated by the LULCC further east, with anomalously low precipitation (Fig. 5h) and soil moisture (Fig. 5i). The drier conditions could result in suppressed dry deposition in the corresponding regions (Fig. 5c). The responses of dry deposition to drought conditions have also been observed by recent studies (e.g., Lin et al., 2019). Furthermore, changes in surface roughness can influence aerodynamic resistance and thus dry deposition via modifying boundary-layer turbulence. In LULCC scenarios, surface roughness is modified substantially with increases in RCP4.5 (Fig. 2j) and reductions in RCP8.5 (Fig. 2o), which generally decrease (increase) resistance and enhance (decrease) dry deposition in RCP4.5 (RCP8.5), though the overall changes in dry deposition is more dominantly shaped by the integrated meteorological effects of LULCC.

Table 2 shows in general, the percentage changes in isoprene emission and dry deposition in the On-line simulations are smaller than in the Off-line simulations in

both scenarios, reflecting that on a global scale, LULCC-induced meteorological changes partly offset the biogeochemical effects of changing land cover types on ozone.

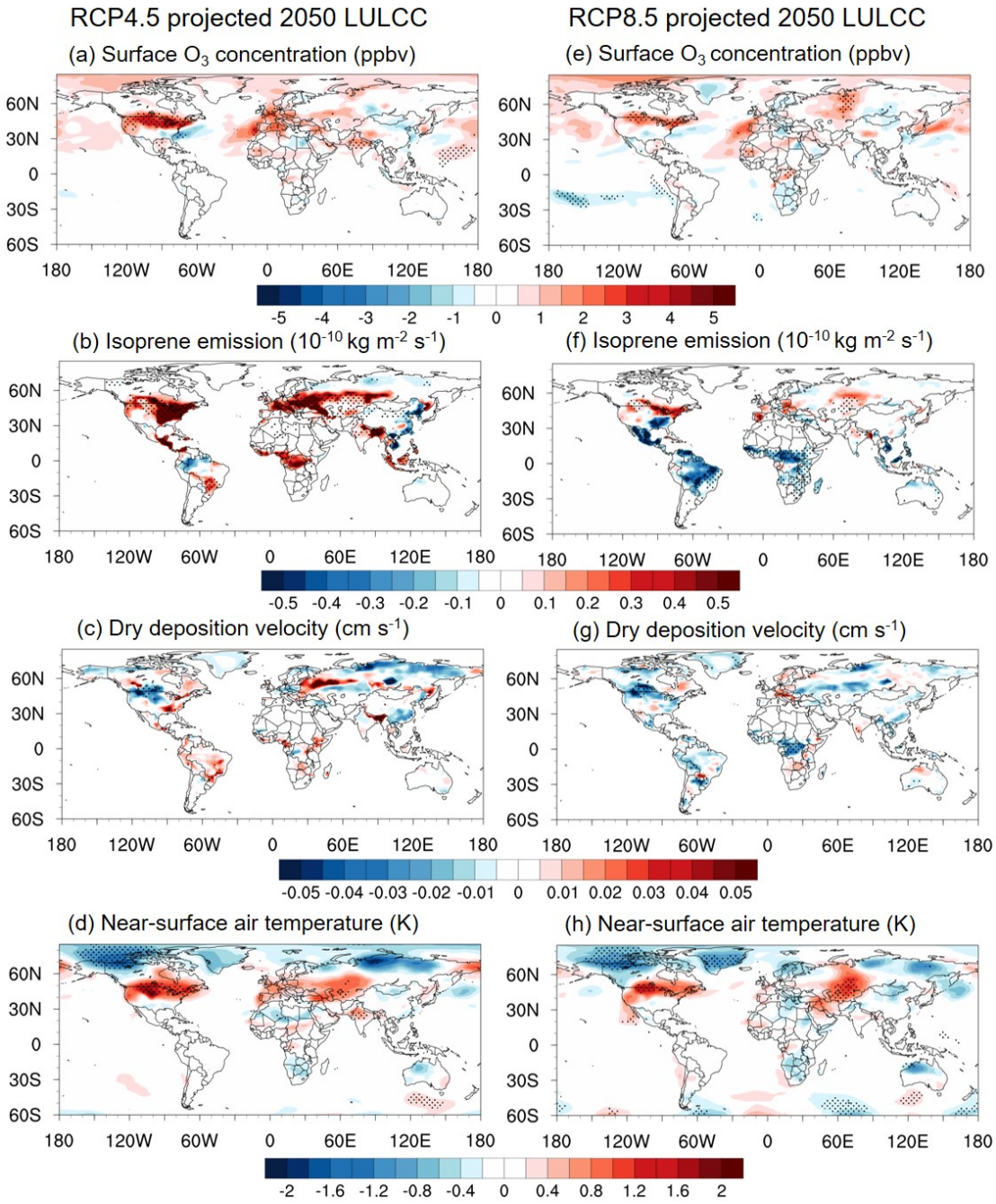

Figure 4. Simulated 2000-to-2050 changes in surface ozone, isoprene emission, dry deposition velocity and near-surface air temperature with atmosphere-chemistry-land coupled configurations for the boreal summer averaged over the 10-year analysis window, under two future scenarios (RCP4.5 and RCP8.5).

Regions with dots indicate changes that are significant at the 90% confidence level. These and all following results are from the On-line runs with dynamic meteorological responses to LULCC.

Thus, changes in ozone can be caused by both biogeochemical and biogeophysical effects of LULCC; furthermore, both effects are highly coupled with each other. We find that in particular the biogeophysical effects of LULCC play critical roles in modulating surface ozone. Hereafter, we focus on the broad regions of North America, Europe and Asia (India and China), in order to elucidate the origins of surface ozone changes in response to LULCC-induced meteorological changes.

3.3.1 North America for RCP4.5 and RCP8.5

For RCP4.5, North America is subjected to intensive local-scale changes in the land cover over the eastern US and southern Canada (Fig. 5d). Relatively large increases in surface ozone (Fig. 4a) and near-surface temperature (Fig. 4d) are found over a large continuous area in North America, including both the region with LULCC and the region where LULCC is minimal. We find that the intensive local-scale LULCC could initiate local temperature change that can further impact larger-scale temperature over North America. For the intensive LULCC region, the eastern US (Fig. 5d), reforestation results in substantial decreases in surface albedo (Fig. 5e), which leads to local increase in surface net solar radiation (Fig. 5f). Reforestation also leads to changes in latent and sensible heat fluxes, as well as surface longwave radiation (not shown here). The net effect is that local temperature increases accordingly. Significant increase of surface temperature is seen over the northeastern US (Fig. 5g). In the southeastern US, surface net solar radiation changes are much smaller, or even negative in some regions (Fig. 5f). Albedo effects of increasing surface net solar radiation appear to be mostly offset by the enhanced precipitation

(Fig. 5h), cloud cover and latent heat, resulting in a modest net cooling at the surface (Fig. 5g).

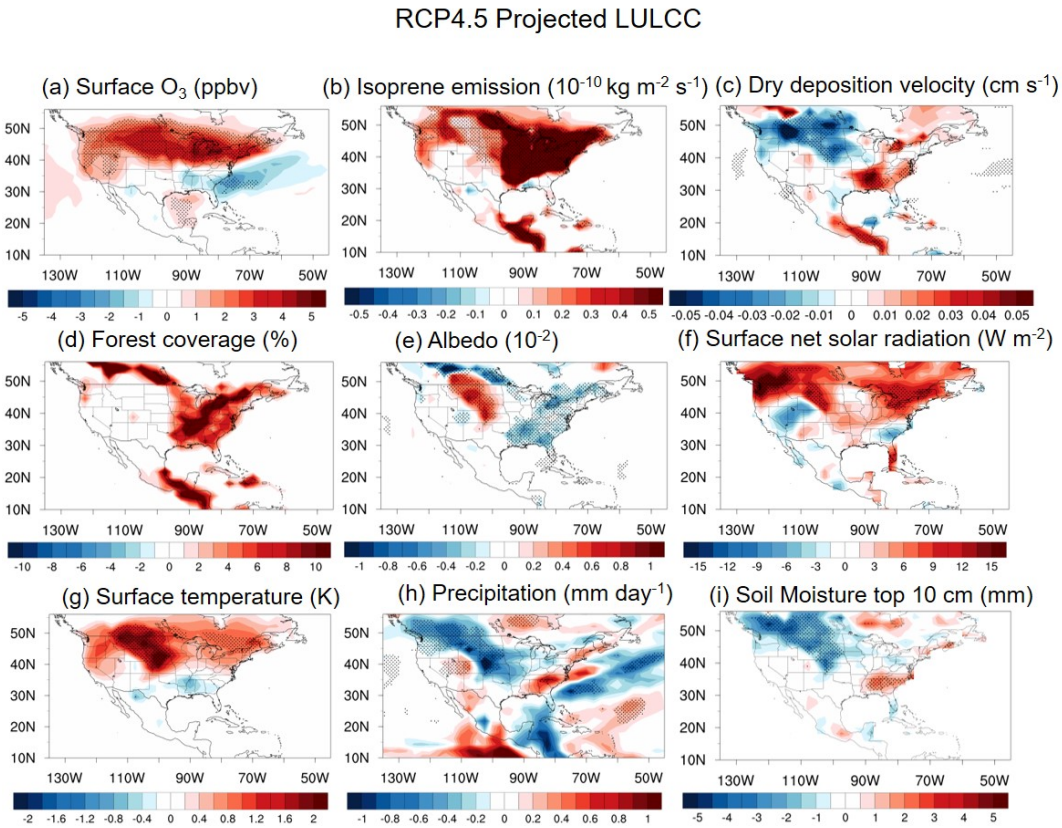

Figure 5. Changes in surface ozone, isoprene emission, dry deposition velocity, projected forest, simulated surface albedo, surface net solar radiation, surface temperature, precipitation, and soil moisture at top 10 cm layer during the boreal summer over the US due to RCP4.5 projected LULCC. Regions with dots indicate changes that are significant at the 90% confidence level.

It is noteworthy that temperature also increases significantly over the locations where the land use does not change, such as the Great Plains and Rocky Mountains in central-western US (Figs. 5d and 5g). The warming over these regions is likely related to atmospheric circulation changes over the northeastern US. Many studies have found that LULCC-induced surface changes can propagate to upper levels vertically and to higher latitudes meridionally (e.g., Chase et al., 2000; Swann et al., 2012; Medvigy, et al., 2013; Xu et al., 2015), resulting in remote effects of LULCC. In our

551 study, surface warming in relation to reduced albedo over the northeastern US can
552 lead to the upper-level warming up to 200 hPa (not shown here). This warming at
553 midlatitudes can lead to anomalous meridional temperature gradient, resulting in the
554 storm track as well as the westerly jet at midlatitudes being displaced northward.
555 Inspection of the anomalous zonal wind at 200 hPa indicates that the westlerly jet
556 core is displaced northward from its climatological position at ~50^{o}N (see Figs. 6a
557 and 6c). Such a displacement of the jet can modulate the local storm track, which can
558 further feedback onto the anomalous flow (Lau, 1988), favoring the formation of an
559 anomalous high immediately to the south at 40-to-50^{o}N over the continental US (Fig.
560 6e). Collocated with such a stationary high, there is enhanced (reduced) surface solar
561 radiation (rainfall and cloud cover). The anomalous high in the RCP4.5 experiment
562 can lead to sinking motion and hence low-level divergent wind that can substantially
563 influence regional moisture transport. The vertically integrated moisture fluxes at
564 present-day conditions are shown in Fig. S3a, illustrating that moisture transport from
565 the Gulf of Mexico and Pacific Ocean is deflected by the Rocky Mountains and
566 toward the central-western US. In fact, the moisture flux pattern is significantly
567 modified in the RCP4.5 runs, such that anomalous moisture flux divergence is found
568 in the region (Fig. S3b). The low-level divergent wind, on the other hand, can also
569 prevent ozone and its precursors along the West Coast from being advected eastward
570 due to the blocking from the Rocky Mountains, resulting in enhanced ozone pollution
571 over the western US. The drier conditions can also be reflected by the anomalously
572 low precipitation (Fig. 5h), lower soil moisture (Fig. 5i) and the associated higher
573 surface albedo (Fig. 5e), which together with the anomalous high (Fig. 6e), can all act
574 to promote warming over the central-western US region.

For the RCP8.5 run, surface ozone is also enhanced in North America (Fig. 4e) and is again well correlated with near-surface warming (Fig. 4h, Fig. S2d). However, the ozone concentration increase is smaller than that in RCP4.5, presumably due to weaker LULCC.

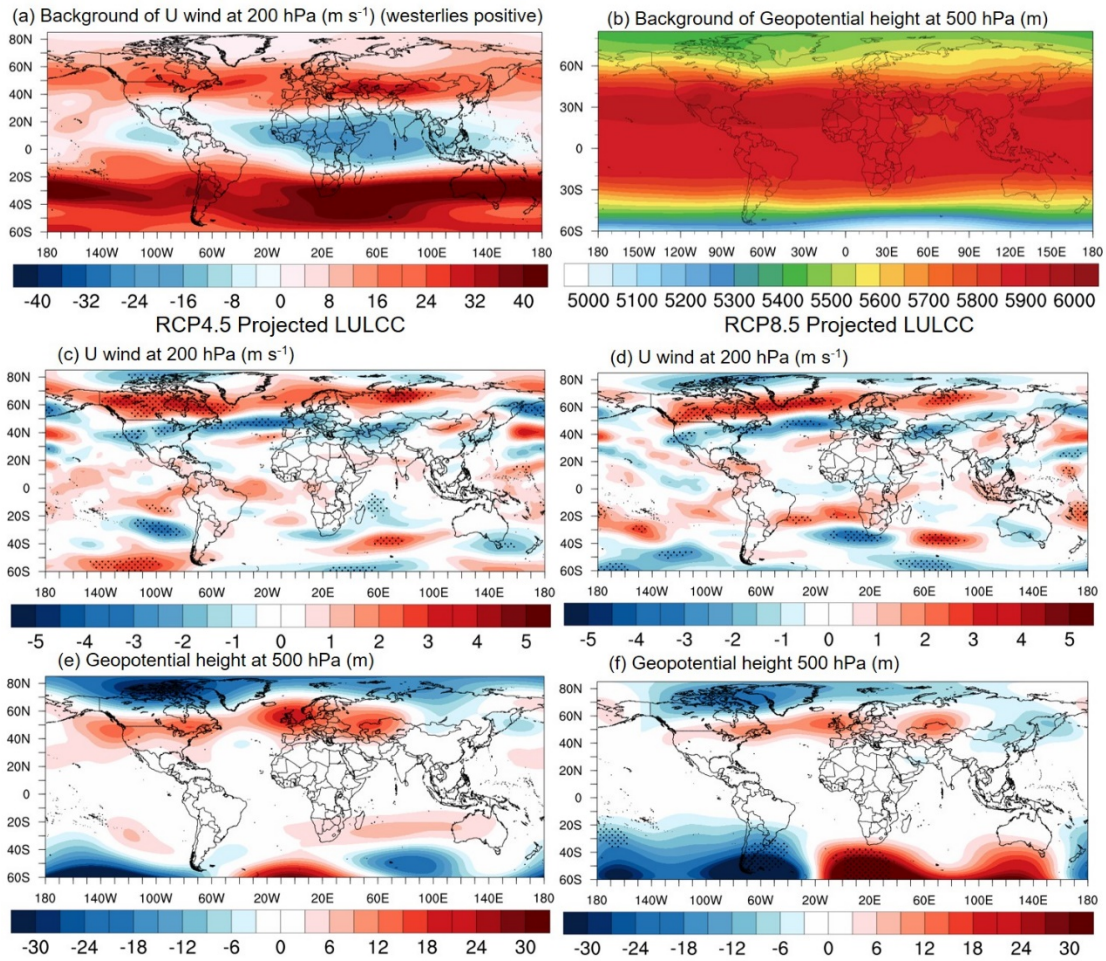

Figure 6. Present-day conditions and changes in zonal wind at 200 hPa and geopotential height at 500 hPa during the boreal summer. Changes due to RCP4.5 projected LULCC change are in middle-bottom left panel, while RCP8.5 in middle-bottom right panel. Regions with dots indicate changes that are significant at the 90% confidence level.

3.3.2 Europe for RCP4.5 and RCP8.5

Along coastal areas of Europe, substantial increases in surface ozone (Figs. 4a, e) and near-surface air temperature (Figs. 4d, h) are found due to RCP4.5 and RCP8.5

LULCC. For RCP4.5, substantial reforestation occurs over Europe continental regions (Fig. 7b), which modifies regional surface energy balance and atmospheric circulation. Forest expansion reduces local albedo (Fig. 7c) and increases surface net solar radiation accordingly over Europe continental areas (Fig. 7d). Reforestation also leads to changes in latent heat and sensible heat fluxes (not shown here). Considering all surface energy components, a positive net heat flux and thus a surface temperature increase are found (Fig. 7e). The higher temperature is seen to be collocated with local surface ozone changes (Fig. 7a) over the continent and coastal regions.

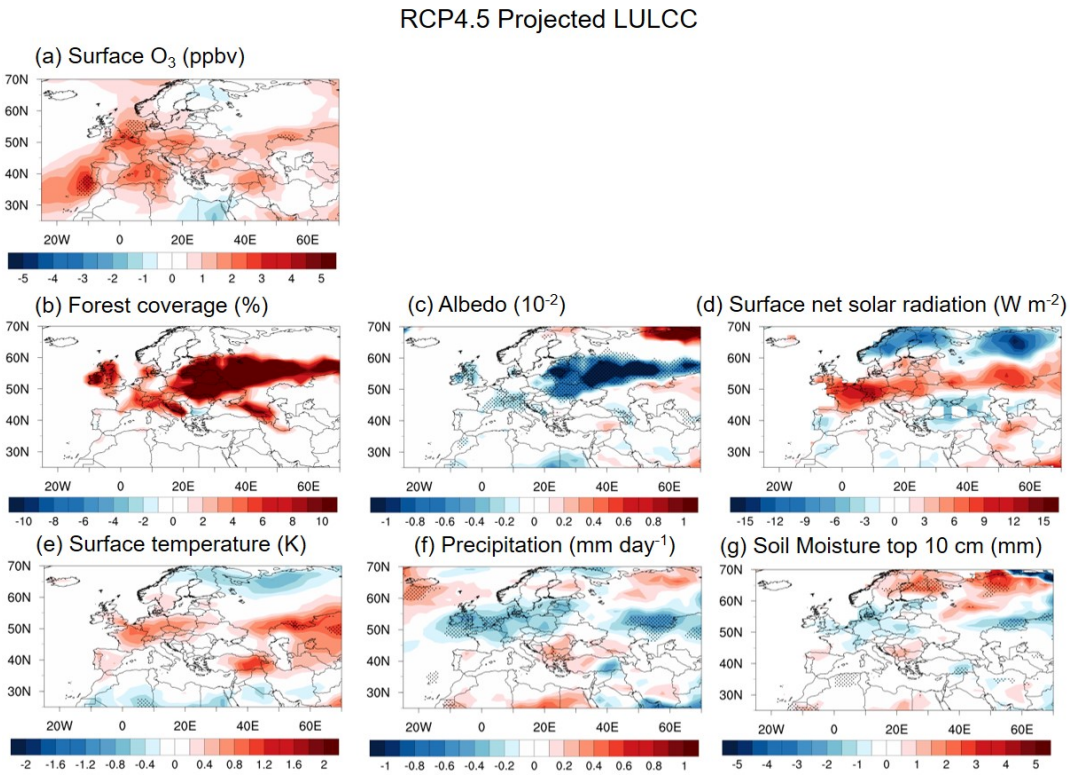

Figure 7. Similar to Figure 5 but for Europe in RCP4.5.

Similar to the anomalous circulation over North America, in Europe there is also surface warming extending to the west of LULCC for RCP 4.5. Again, this is likely due to a similar mechanism in which the northward-migrating storm track (Fig. 7f) and westerlies (Fig. 6c) are found at about 55–60°N; modified storm tracks and the

anomalous high are acting in concert, leading to more subsidence in the European region that experiences increased surface net solar radiation (Fig. 7d), thus surface warming (Fig. 7e). For RCP8.5, reforestation occurs over limited areas of Europe (Figs. 2l); similar changes in the local climate and surface ozone are found, albeit with a relatively weak amplitude compared with their RCP8.5 counterparts.

3.3.3 India and China for RCP4.5 and RCP8.5

For RCP4.5, extensive reforestation occurs in northeastern and southwestern India (Fig. 8b). There is also a significant increase of surface ozone over northern India (Fig. 4a), collocated with warming (Fig. 4d). Again, temperature increase tends to occur west of the LULCC (Fig. 8e). The LULCC-induced lower albedo (Fig. 8c) and higher net surface solar radiation (Fig. 8d) cause more energy to be absorbed by the land surface at high elevations and warm the overlying air accordingly. Again, the rainbelt is displaced northward, likely reflecting perturbed synoptic-scale activities in the region. Consistent with the former feature, the mid-tropospheric anomalous flow is characterized by an anticyclone between 20–30^{o}N, suppressing rainfall therein (Figs. 8f, 8g). The anomalous anticyclone in turn can lead to more surface net radiation in northern India as a remote effect (Fig. 8d). Thus, in northern India there is significant surface warming (Fig. 8e) and enhanced surface ozone.

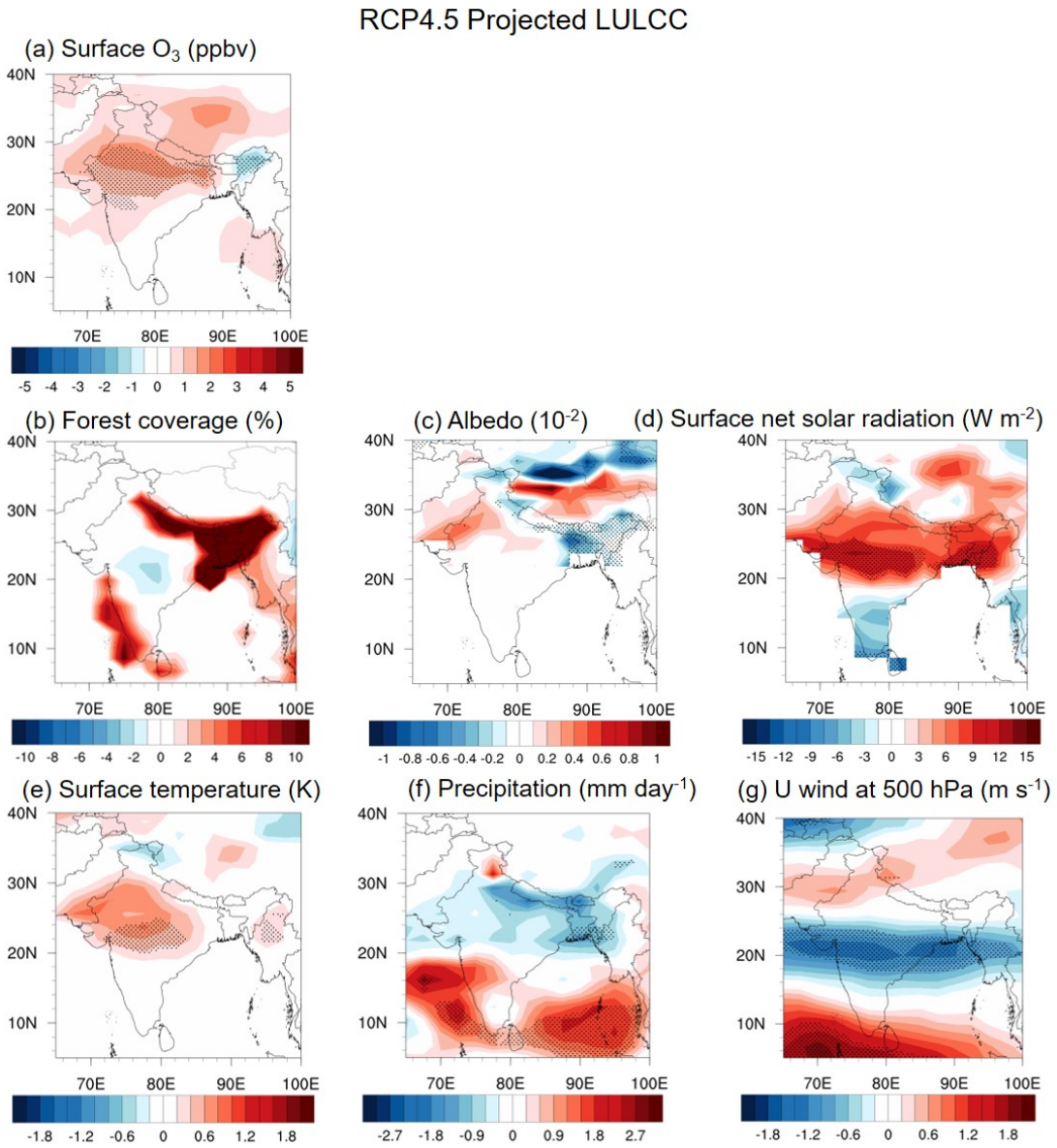

Figure 8. Similar to Figure 5 but for India in RCP4.5.

Finally, in China extensive deforestation occurs for RCP4.5 (Fig. 2f). Surface ozone shows a slightly decrease (Fig. 4a) that could be caused by biogeochemical effects associated with LULCC instead of biogeophysical effects. This region is characterized by a temperate climate, medium isoprene emission from temperate trees (Fig. 3a) and high anthropogenic NO_x emissions. Changes from temperate trees to croplands further decrease isoprene emission and lead to significant ozone decreases, which largely offsets the effects of reduced dry deposition velocity (Fig. 4b). For

RCP8.5, little change in surface ozone or temperature has been found in either country.

Overall, we find that biogeophysical effects can have strong impacts on surface ozone through modifying local and remote meteorological conditions such as surface warming and circulation anomalies initiated by local LULCC (Fig. 1). Our results of temperature changes are consistent with the previous study of Swann et al. (2012) that illustrated the local and remote climate effects of the northern midlatitude reforestation. They conducted a model experiment with extreme afforestation, and found substantial warming in North America and Europe. In addition, Govindasamy and Caldeira (2001) and Unger (2014) also found surface cooling due to deforestation.

3.3.4 Time-sliced experiments versus transient experiments

In the Off-line configurations, we use time-sliced experiments for present-day land cover conditions in 2000 and future conditions in 2050. However, the LULCC in On-line mode is transient with the land cover changing annually and the atmosphere responds to such changes accordingly. For a paralleled comparison with Off-line mode, time- sliced runs in On-line mode are also conducted. Our results show that changes in ozone, near-surface air temperature, and other factors controlling ozone are similar between transient and time-sliced runs in the On-line mode (Fig. 9 and Table 2). The consistent model performance using transient and time-sliced LULCC indicates that the LULCC-forced signal is strong enough to cause changes in meteorology and ozone pollution, and the atmospheric responses and the biogeophysical effects are generally fast-responding at a quasi-steady state on timescales of years to decades with respect to the slow LULCC.

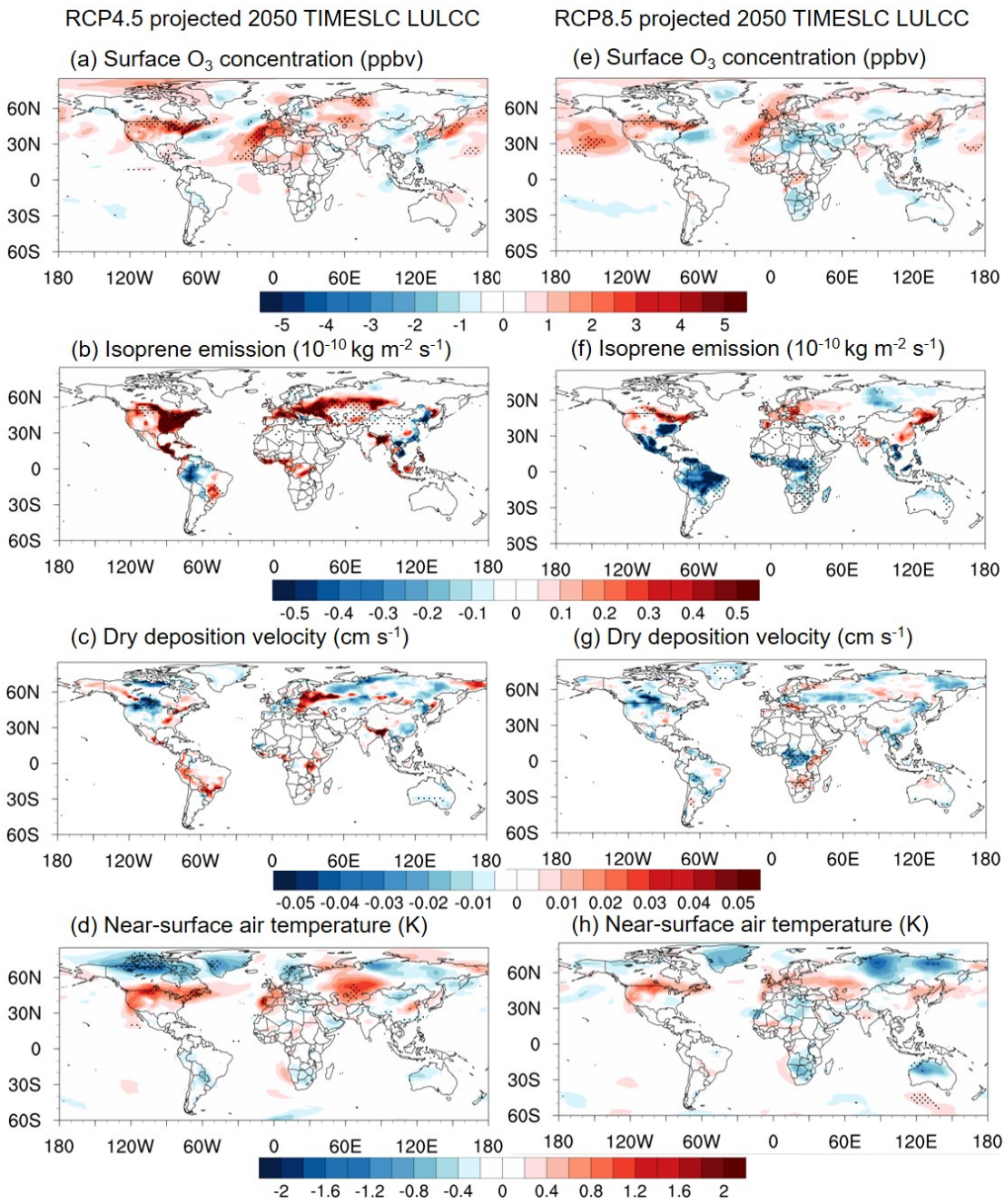

Figure 9. Similar to Figure 4 but simulated from time-sliced configurations.

4. Conclusions and Discussion

LULCC is expected to continue to co-occur with future socioeconomic development and anthropogenic emission reduction strategies. These changes likely had, and will continue to have a large impact on air quality and climate. However, the impacts of LULCC on surface ozone pollution are not fully understood, and the

attribution to different LULCC-mediated pathways is far from complete. Here, we investigate and quantify specifically the biogeochemical effects (via modifying ozone-relevant chemical fluxes), biogeophyscial effects (via modifying the overlying meteorological environment), and the integrated effects of LULCC on surface ozone air quality.

We address the biogeochemical effects alone by performing CESM simulations with prescribed meteorology, and investigate the integrated effects using atmosphere-chemistry-land coupled configuration with dynamic meteorology. We find that the biogeochemical effects of changing isoprene emission and dry deposition following LULCC mostly offset each other, resulting in only modest changes in ozone by up to 2 ppbv from 2000 to 2050. However, surface ozone can be significantly altered by up to 6 ppbv when considering the integrated effects associated with the LULCC. In particular, the biogeophysical effects facilitated through temperature changes plays a critical role in shaping surface ozone. We find that temperature and surface ozone increase significantly in RCP4.5 over both regions with intensive LULCC, such as the northeastern US, continental Europe and northeastern India, and regions with limited LULCC, such as the central-western US, coastal Europe and northwestern India.

The surface ozone changes due to future LULCC are comparable with anthropogenic emissions and climate, and thus should be taken into account in future research and policy planning. For example, summertime surface ozone changes induced by climate change alone are projected to increase by 1–10 ppb in the US, Europe, East and South Asia (e.g., Jacob and Winner, 2009; Fiore et al., 2012). It is also found that the combined effects of changing climate, emissions and land cover on surface ozone are up to 10 ppb in the US under two RCP scenarios, and the

688 contributions from the three factors have comparable magnitudes although of
689 different signs (Val Martin, et al., 2015). Wang et al. (2011) found that in China,
690 summertime surface ozone decreases by ~10 ppb on average with a maximum
691 reduction of 25 ppb if all anthropogenic emissions are removed. Our simulated ozone
692 changes induced by LULCC are substantial and within the same order of magnitude
693 as the above studies and others that considered meteorological responses to LULCC
694 (Ganzeveld et al., 2010; Val Martin et al., 2015). This highlights the important roles
695 of LULCC in modulating surface ozone.

696 The mechanisms behind temperature responses to LULCC can be as follows:
697 first, surface properties (e.g., surface albedo, evapotranspiration, and surface
698 roughness) are altered; the changes in surface properties lead to changes in surface
699 energy budget and surface temperature locally; then these changes would propagate to
700 upper levels of the atmosphere and further induce a regional circulation response, in
701 particular the formation of anomalous stationary high-pressure systems and warming
702 conditions over the mid-to-high northern latitudes in boreal summer as a remote
703 effect. Meanwhile, the anomalous high diverges moisture transport away from the
704 region, inducing a series of feedbacks that result in generally drier and warmer
705 conditions (Fig. 1).

706 Weaker responses of temperature as well as of surface ozone to LULCC are
707 found in RCP8.5 compared with those in RCP4.5. The different extent of temperature
708 responses can be attributed to the location where LULCC occurs. For RCP4.5,
709 LULCC is most intense in the mid-latitude region of NH. In contrast, most LULCC
710 for RCP8.5 occurs over the equatorial regions and Southern Hemisphere (SH).
711 Temperature responses to LULCC may be less sensitive to tropical changes or
712 changes over SH that is dominated by the vast oceanic expanse. Van der Molen et al

(2011) using other models also found similar patterns, and named such climate responses to LULCC as “tropical damping”. The classical theory of such “tropical damping” is associated with a decrease in cloud cover after deforestation, which then results in increased incoming radiation at the surface and a lower planetary albedo, both counteracting the increase in surface albedo with deforestation. A similar northward displacement of the jet stream in the RCP4.5 and RCP8.5 simulations is also found, despite quite different LULCC patterns on a regional scale; this indicates that the mostly extratropical afforestation in RCP4.5 vs. the mostly tropical deforestation in RCP8.5 can lead to similar hemispheric-scale circulation changes that likely reflects common connections to the warming at midlatitudes.

Our study has several limitations. First, the energy transport between the ocean and land has not been taken into account. Although using a fully interactive ocean component would increase the variability of simulated climate and decrease the signal-to-noise ratio in sensitivity experiments using small forcings, such as LULCC (e.g., Davin and de Noblet-Ducoudre 2010, Brovkin et al., 2013), coupled atmosphere-ocean simulations are crucial for future climate change projections for the longer term (e.g., well past the end of the 21st century). In addition, future LULCC projections in RCPs are predicted from the ensemble of socioeconomic and emission scenarios to match identified pathways of greenhouse gas concentrations. Large uncertainties remain in such projections, calling for more skillful design of LULCC-related metrics and the corresponding spatial patterns for better air quality predictions. Third, the biogeochemical effects of LULCC on ozone in this study do not consider climatic changes or anthropogenic emission change, but only focus on the more immediate effects generated from LULCC such as isoprene emission and dry deposition, mostly due to model limitations. For example, NO_x emission is projected

738 to decline sharply over the northeastern US in RCP4.5. As NO_x level decreases, ozone
739 production may become more NO_x-limited and thus the sensitivity to isoprene
740 emission may be reduced, rendering the overall biogeochemical effects of LULCC
741 smaller. However, since the biogeophysical effects operate in locations remote from
742 the source regions, they may be less affected by NO_x emission changes in the source
743 regions. The full biogeochemical effects of LULCC on ozone that include
744 biogeochemical cycle-climate feedbacks and co-effects of anthropogenic emission
745 and LULCC will warrant further investigation but will foreseeably present greater
746 challenges for process attribution and interpretation.

747 Atmospheric internal variability is one factor that could affect the significance
748 of our results. Large internal variability of the climate system reduces the signal-to-
749 noise ratio for LULCC-induced climatic changes. This is analogous to the problem of
750 long-term low-frequency variability of the extratropical circulation affecting the
751 interpretation and extraction of climate change signals, especially if short time series
752 (e.g., ~10 years) are used (Deser et al., 2012). When applicable, multiple-member
753 ensemble runs are required to ascertain the impacts of such variability. Our model
754 experiments with a 55-year transient integration with prescribed sea surface
755 temperature and sea ice are not designed to address such low-frequency climate
756 variability. We note however that our climate simulations focus on land-atmosphere
757 biogeophysical interactions, which typically operate on a shorter timescale, and thus
758 the LULCC-induced climate signals that we detected are expected be present when
759 superimposed upon any long-term trajectory and low-frequency variability undergone
760 by the climate system. For land-atmosphere interactions, high-frequency interannual
761 variability on a decadal timescale may be more relevant. To assess the potential
762 impacts of the internal variability of the system on a decadal timescale, we have

compared the magnitudes of interannual standard deviations of near-surface temperature of the CTL run with the LULCC-induced climate signals. Our results show that the climate signals are not weak and can be comparable to interannual variability at midlatitudes (Fig. S4), e.g., over North America land areas at ~45°N and also north of 60°N. It is also noteworthy that the time-sliced experiments with single-year forcing looped for multiple years, give results very similar to the transient simulations, pointing to the robustness of LULCC impacts.

Our study highlights the complexity of land surface forcing and the importance of biogeophysical effects of LULCC on surface ozone air quality, emphasizing the importance of LULCC in shaping atmospheric chemistry that could be as important as anthropogenic emissions and climate. Our study can provide important reference for policy makers to consider the substantial roles of LULCC in tackling air pollution and climate change, to develop a more comprehensive set of climatically relevant metrics for the management of the terrestrial biosphere, as well as to explore co-benefits among air pollution, climate change and land use management strategies.

Author Contribution

L. Wang designed the model experiments, performed numerical simulations and analysis, and co-wrote the manuscript; A. P. K. Tai and C.-Y. Tam are the co-principal investigators, who designed the research, performed some of the analysis, and co-wrote the manuscript; and all authors contributed to the interpretation of the results and writing of the paper.

Acknowledgments

This work was supported by the Vice-Chancellor Discretionary Fund (Project ID: 4930744) from The Chinese University of Hong Kong (CUHK) given to the Institute of Environment, Energy and Sustainability. It is also supported by a General Research Fund grant (Project ID: 14306015) from the Research Grants Council of Hong Kong given to A. P. K. Tai.

References

Arora, V. K., and Montenegro, A.: Small temperature benefits provided by realistic afforestation efforts. Nat. Geosci., 4, 514-518. https://doi.org/10.1038/ngeo1182, 2011.

Avnery S., Mauzerall D. L., Liu J., and Horowitz L. W.: Global crop yield reductions due to surface ozone exposure: 2. Year 2030 potential crop production losses and economic damage under two scenarios of O_3 pollution, Atmos. Environ., 45, 2297-2309, https://doi.org/10.1016/j.atmosenv.2011.01.002, 2011.

Betts, R. A.: Biogeophysical impacts of land use on present-day climate: near-surface temperature change and radiative forcing, Atmos. Sci. Lett., 2, 39-51, https://doi.org/10.1006/asle.2001.0023, 2001.

Boisier, J. P., de Noblet-Ducoudré, N., Pitman, A. J., Cruz, F. T., Delire, C., van den Hurk, B. J. J. M., . . . Voldoire, A.: Attributing the impacts of land-cover changes in temperate regions on surface temperature and heat fluxes to specific causes: Results from the first LUCID set of simulations. Journal of Geophysical Research: Atmospheres, 117, D12. https://doi.org/10.1029/2011JD017106, 2012.

Bonan, G. B.: Forests and climate change: Forcings, feedbacks, and the climate benefits of forests. Science, 320, 1444-1449, https://doi.org/10.1126/science.1155121, 2008.

Bonan, G.: Forests, Climate, and Public Policy: A 500-Year Interdisciplinary Odyssey, Annu. Rev. Ecol. Evol. Syst., 47, 97-121, https://doi.org/10.1146/annurev-ecolsys-121415-032359, 2016.

Brovkin, V., Boysen L., Arora, V. K., Boisier, J. P., Cadule, P., Chini, L., Claussen, M., Friedlingstein, P., Gayler, V., van den Hurk, B. J. J. M., Hurtt, G. C., Jones, C. D., Kato, E., de Noblet-Ducoudré, N., Pacifico, F., Pongratz, J., and Weiss, M.: Effect of

anthropogenic land-use and land-cover changes on climate and land carbon storage in CMIP5 projections for the twenty-first century, J. Clim., 26, 6859-6881, https://doi.org/10.1175/JCLI-D-12-00623.1, 2013.

Brown-Steiner, B., Hess, P. G., and Lin, M. Y.: On the capabilities and limitations of GCCM simulations of summertime regional air quality: A diagnostic analysis of ozone and temperature simulations in the US using CESM CAM-Chem, Atmospheric Environment, 101, 134-148, https://doi.org/10.1016/j.atmosenv.2014.11.001, 2015.

Chase, T., Pielke, R., Kittel, T., Nemani, R., and Running, S.: Simulated Impacts of Historical Land Cover Changes on Global Climate in Northern Winter, Clim. Dynam., 16, 93-105, https://doi.org/10.1007/s003820050007, 2000. .

de Noblet-Ducoudré, N., Boisier, J. P., Pitman, A., Bonan, G. B., Brovkin, V., Cruz, F., …Voldoire, A.: Determining robust impacts of land-use-induced land cover changes on surface climate over North America and Eurasia: Results from the first set of LUCID experiments. J. Clim., 25, 3261-3281. https://doi.org/10.1175/JCLI-D-11-00338.1, 2012.

Deser, C., Knutti, R., Solomon, S., Phillips, A.: Communication of the role of natural variability in future North American Climate. Nature Clim. Change, 2, 775-779, doi:10.1038/nclimate1562, 2012.

Devaraju, N., Bala, G., Modak, A.: Effects of large-scale deforestation on precipitation in the monsoon regions: Remote versus local effects. PNAS, 112, 3257-3262, doi:10.1073/pnas.1423439112, 2015.

Doherty, R. M., Wild, O., Shindell, D. T., Zeng, G., MacKenzie, I. A., Collins, W. J., Fiore, A. M., Stevenson, D. S., Dentener, F. J., Schultz M. G., Hess, P., Derwent, R. G., and Keating, T. J.: Impacts of climate change on surface ozone and

844 intercontinental ozone pollution: A multi-model study, J. Geophys. Res. Atmos., 118,
845 1-20, https://doi.org/10.1002/jgrd.50266, 2013.
846 Emmons, L. K., Walters, S., Hess, P. G., Lamarque, J.-F., Pfister, G. G., Fillmore, D.,
847 Granier, C., Guenther, A., Kinnison, D., Laepple, T., Orlando, J., Tie, X., Tyndall, G.,
848 Wiedinmyer, C., Baughcum, S. L., and Kloster, S.: Description and evaluation of the
849 Model for Ozone and Related chemical Tracers, version 4 (MOZART-4), Geosci.
850 Model Dev., 3, 43-67, https://doi.org/10.5194/gmd-3-43-2010, 2010.
851 Fiore, A. M., Horowitz, L. W., Purves, D. W., Levy II, H., Evans, M. J., Wang, Y.,
852 Li, Q., and Yantosca, M.: Evaluating the contribution of changes in isoprene
853 emissions to surface ozone trends over the eastern United States, J. Geophys. Res.
854 Atmos., 110, D12303, https://doi.org/10.1029/2004JD005485, 2005.
855 Fiore, A. M., Naik, V., Spracklen, D. V., Steiner, A., Unger, N., Prather, M., and
856 Bergmann, D.: Global air quality and climate, Chem. Soc. Rev., 41, 6663-6683, DOI:
857 10.1039/C2CS35095E, 2012.
858 Fu, Y., and Tai, A. P. K.: Impact of climate and land cover changes on tropospheric
859 ozone air quality and public health in East Asia between 1980 and 2010, Atmos.
860 Chem. Phys., 15, 10093-10106, https://doi.org/10.5194/acp-15-10093-2015, 2015.
861 Ganzeveld, L., Bouwman, L., Stehfest, E., van Vuuren, D. P., Eickhout, B., and
862 Lelieveld, J.: Impact of future land use and land cover changes on atmospheric
863 chemistry-climate interactions, J. Geophys. Res. Atmos., 115, D23301,
864 https://doi.org/10.1029/2010JD014041, 2010.
865 Govindasamy, B., and Caldeira, K.: Land use changes and Northern Hemisphere
866 cooling, Geophys. Res. Lett., 28, 291-294, https://doi.org/10.1029/2000GL006121,
867 2001.

868 Guenther, A. B., Jiang, X., Heald, C. L., Sakulyanontvittaya, T., Duhl, T., Emmons,
869 L. K., and Wang, X.: The Model of Emissions of Gases and Aerosols from Nature
870 version 2.1 (MEGAN2.1): an extended and updated framework for modeling biogenic
871 emissions, Geosci. Model Dev., 5, 1471-1492, https://doi.org/10.5194/gmd-5-1471-
872 2012, 2012.
873 Henderson-Sellers, A., Dickinson, R. E., Durbidge, T. B., Kennedy, P. J., McGuffie,
874 K., and Pitman, A. J.: Tropical deforestation: Modeling local- to regional-scale
875 climate change, J. Geophys. Res. Atmos., 98, 7289-7315,
876 https://doi.org/10.1029/92JD02830, 1993.
877 Heald C. L., Henze, D. K., Horowitz, L. W., Feddema, J., Lamarque, J. ‐ F.,
878 Guenther, A., Hess, P. G., Vitt, F., Seinfeld, J. F., Goldstein, A. H., and Fung, I.:
879 Predicted change in global secondary organic aerosol concentrations in response to
880 future climate, emissions, and land use change, J. Geophys. Res., 113, D05211,
881 doi:10.1029/2007JD009092, 2008.
882 Heald, C. L., and Spracklen, D. V.: Land use change impacts on air quality and
883 climate, Chem. Rev., 115, 4476-4496, https://doi.org/10.1021/cr500446g, 2015.
884 Heald, C. L., and Geddes, J. A.: The impact of historical land use change from 1850
885 to 2000 on secondary particulate matter and ozone, Atmos. Chem. Phys., 16, 14997-
886 15010, https://doi.org/10.5194/acp-16-14997-2016, 2016.
887 Hurtt, G. C., Chini, L. P., Frolking, S., Betts, R. A., Feddema, J., Fischer, G., Fisk, J.
888 P., Hibbard, K., Houghton, R. A., Janetos, A., Jones, C. D., Kindermann, G.,
889 Kinoshita, T., Goldewijk, K. K., Riahi, K., Shevliakova, E., Smith, S., Stehfest, E.,
890 Thomson, A., Thornton, P., van Vuuren, D. P., and Wang, Y. P.: Harmonization of
891 land-use scenarios for the period 1500–2100: 600 years of global gridded annual land-

use transitions, wood harvest, and resulting secondary lands, Climatic Change, 109, 117-161, DOI:10.1007/s10584-011-0153-2, 2011.

Jacob, D. J., and Winner, D. A.: Effect of climate change on air quality, Atmos. Environ., 43, 51-63, https://doi.org/10.1016/j.atmosenv.2008.09.051, 2009.

Jerrett, M., Burnett, R. T., Pope, C. A., Ito, K., Thurston, G., Krewski, D., Shi, Y., Calle, E., and Thun, M.: Long-Term Ozone Exposure and Mortality, New Engl. J. Med., 360, 1085-1095, DOI: 10.1056/NEJMoa0803894, 2009.

Jiang, X., Wiedinmyer, C., Chen, F., Yang, Z.-L., and Lo, J. C.-F.: Predicted impacts of climate and land use change on surface ozone in the Houston, Texas, area, J. Geophys. Res., 113, D20312, https://doi.org/10.1029/2008JD009820, 2008.

Kang, D., Aneja, V. P., Mathur, R., and Ray, J. D.: Nonmethane hydrocarbons and ozone in three rural southeast United States national parks: A model sensitivity analysis and comparison to measurements, J. Geophys. Res., 108, 4604, https://doi.org/10.1029/2002JD003054, 2003.

Kubistin, D., Harder, H., Martinez, M., Rudolf, M., … , and Lelieveld, J. Hydroxyl radicals in the tropical troposphere over the Suriname rainforest: comparison of measurements with the box model MECCA. Atmos. Chem. Phys., 10, 9705-9728, 2010. doi:10.5194/acp-10-9705-2010.

Lamarque, J.-F., Bond, T. C., Eyring, V., Granier, C., Heil, A., Klimont, Z., Lee, D., Liousse, C., Mieville, A., Owen, B., Schultz, M. G., Shindell, D., Smith, S. J., Stehfest, E., Van Aardenne, J., Cooper, O. R., Kainuma, M., Mahowald, N., McConnell, J. R., Naik, V., Riahi, K., and van Vuuren, D. P.: Historical (1850-2000) gridded anthropogenic and biomass burning emissions of reactive gases and aerosols: methodology and application, Atmos. Chem. Phys., 10, 7017-7039, https://doi.org/10.5194/acp-10-7017-2010, 2010.

Lamarque, J. F., Emmons, L. K., Hess, P. G., Kinnison, D. E., Tilmes, S., Vitt, F., Heald, C. L., Holland, E. A., Lauritzen, P. H., Neu, J., Orlando, J. J., Rasch, P. J., and Tyndall, G. K.: CAM-chem: description and evaluation of interactive atmospheric chemistry in the Community Earth System Model, Geosci. Model Dev., 5, 369-411, https://doi.org/10.5194/gmd-5-369-2012, 2012.

Laguë, M., and Swann, A. S.: Progressive midlatitude afforestation: Impacts on clouds, global energy transport, and precipitation. J. Clim., 29, 5561-5573, https://doi.org/10.1175/JCLI-D-15-0748.1, 2016.

Laguë, M. M., Bonan, G. B., Swann, A. S.: Separating the impact of individual land surface properties on the terrestrial surface energy budget in both the coupled and un-coupled land-atmosphere system. J. Clim. Preprint. 2019.

Lapina, K., Henze, D. K., Milford, J. B., Huang, M., Lin, M., Fiore, A. M., Carmichael, G., Pfister, G. G., and Bowman, K.: Assessment of source contributions to seasonal vegetative expo- sure to ozone in the US, J. Geophys. Res. Atmos., 119, 324-340, https://doi.org/10.1002/2013JD020905, 2014.

Lathière, J., Hauglustaine, D. A., Friend A. D., de Noblet-Ducoudré, N., Viovy N., and Folberth, G. A.: Impact of climate variability and land use changes on global biogenic volatile organic compound emissions, Atmos. Chem. Phys., 6, 2129-2146, https://doi.org/10.5194/acp-6-2129-2006, 2006.

Lawrence, D. M., Oleson, K. W., Flanner, M. G., Thornton, P. E., Swenson, S. C., Lawrence, P. J., Zeng, X., Yang, Z.-L., Levis, S., Sakaguchi, K., Bonan, G. B., and Slater, A. G.: Parameterization Improvements and Functional and Structural Advances in Version 4 of the Community Land Model, J. Adv. Model. Earth Syst., 3, M03001, https://doi.org/10.1029/2011MS00045, 2011.

941 Lawrence, P. J., Feddema, J. J., Bonan, G. B., Meehl, G. A., O'Neill, B. C., Levis, S.,
942 Lawrence, D. M., Oleson, K. W., Kluzek, E., Lindsay, K., and Thorton, P. E.:
943 Simulating the Biogeochemical and Biogeophysical Impacts of Transient Land Cover
944 Change and Wood Harvest in the Community Climate System Model (CCSM4) from
945 1850 to 2100, J. Climate., 25, 3071-3095, https://doi.org/10.1175/JCLI-D-11-00256.1,
946 2012.
947 Lau, N.-C.: Variability of the observed midlatitude storm tracks in relation to low-
948 frequency change in the circulation pattern, J. Atmos. Sci., 45, 2718-2743,
949 https://doi.org/10.1175/1520-0469(1988)045<2718:VOTOMS>2.0.CO;2, 1988.
950 Lin, M., Horowitz, L. W., Payton, R., Fiore, A. M., and Tonnesen G.: US surface
951 ozone trends and extremes from 1980 to 2014: quantifying the roles of rising Asian
952 emissions, domestic controls, wildfires, and climate, Atmos. Chem. Phys., 17, 2943-
953 2970, https://doi.org/10.5194/acp-17-2943-2017, 2017.
954 Lin, M., Malyshev, S., Shevliakova, E., and co-authors. Sensitivity of ozone dry
955 deposition to ecosystem-atmosphere interactions: A critical appraisal of observations
956 and simulations, Global Biogeochemical Cycles, 33, 1264-1288,
957 https://doi.org/10.1029/2018GB006157, 2019.
958 Lee, X., Goulden, M. L., Hollinger, D. Y., Barr, A., Black, T. A., Bohrer, G., …Zhao,
959 L. Observed increase in local cooling effect of deforestation at higher latitudes.
960 Nature, 479, 384-387. https://doi.org/10.1038/nature10588, 2011.
961 Malley, C. S., Henze, D. K., Kuylenstierna, J. C. I., Vallack, H. W., Davila, Y.,
962 Anenberg, S. C., Turner, M. C., and Ashmore, M. R.: Updated global estimates of
963 respiratory mortality in adults ≥30 years of age attributable to long-term ozone
964 exposure, Environ, Health Perspect., 125, 087021, doi: 10.1289/EHP1390, 2017.

965 Medvigy, D., Walko, R., Otte, M., and Avissar, R. Simulated Changes in Northwest
966 U.S. Climate in Response to Amazon Deforestation. J. Climate, 26, 9115-9136,
967 https://doi.org/10.1175/JCLI-D-12-00775.1, 2013.
968 Myhre, G., et al.: Anthropogenic and Natural Radiative Forcing. In: Climate Change
969 2013: The Physical Science Basis. Contribution of Working Group I to the Fifth
970 Assessment Report of the Intergovernmental Panel on Climate Change (Stocker, T.F.,
971 et al., (eds.)). Cambridge University Press, Cambridge, United Kingdom and New
972 York, NY, USA, 2013.
973 Oleson, K. W., Lawrence D. W., and Bonan, G. B.: Technical description of version
974 4.5 of the Community Land Model (CLM). NCAR Technical Note NCAR/TN-
975 503+STR, National Centre for Atmospheric Research, Boulder, USA, 2013.
976 Parrish, D. D., Lamarque, J. F., Naik, V., Horowitz, L., Shin- dell, D. T., Staehelin, J.,
977 Derwent, R., Cooper, O. R., Tanimoto, H., Volz-Thomas, A., and Gilge, S.: Long-
978 term changes in lower tropospheric baseline ozone concentrations: Comparing
979 chemistry-climate models and observations at northern midlatitudes, J. Geophys. Res.
980 Atmos., 119, 5719-5736, https://doi.org/10.1002/2013JD021435, 2014.
981 Pfister, G. G., Emmons, L. K., Hess, P. G., Lamarque, J.-F., Orlando, J. J., Walters,
982 S., Guenther, A., Palmer, P. I., and Lawrence, P. J.: Contribution of isoprene to
983 chemical budgets: A model tracer study with the NCAR CTM MOZART-4, J.
984 Geophys. Res., 113, D05308, https://doi.org/10.1029/2007JD008948, 2008.
985 Pitman, A. J., de Noblet-Ducoudre, N., Cruz, F. T., Davin, E. L., Bonan, G. B.,
986 Brovkin, V., Claussen, M., Delire, C., Ganzeveld, L., Gayler, V., van den Hurk, B.,
987 Lawrence, P. J., van der Molen, M. K., Muller, C., Reick, C. H., Seneviratne, S. I.,
988 Strengers, B. J., and Voldoire, A.: Uncertainties in climate responses to past land

989 cover change: First results from the LUCID intercomparison study, Geophys. Res.
990 Lett., 36, L14814, https://doi.org/10.1029/2009GL039076, 2009.
991 Porter, W. C., Heald, C. L., Cooley, D., and Russell, B.: Investigating the observed
992 sensitivities of air-quality extremes to meteorological drivers via quantile regression,
993 Atmos. Chem. Phys., 15, 10349-10366, https://doi.org/10.5194/acp-15-10349-2015,
994 2015.
995 Pusede, S. E., Steiner, A. L., and Cohen, R. C.: Temperature and recent trends in the
996 chemistry of continental surface ozone, Chem. Rev., 115, 3898-3918,
997 https://doi.org/10.1021/cr5006815, 2015.
998 Rayner, N. A., Parker, D. E., Horton, E. B., Folland, C. K., Alexander, L. V., Rowell,
999 D. P., Kent, E. C., and Kaplan, A.: Global analyses of sea surface temperature, sea
1000 ice, and night marine air temperature since the late nineteenth century, J. Geophys.
1001 Res. Atmos., 108, D002670, https://doi.org/10.1029/2002JD002670, 2003.
1002 Riahi, K., Grübler, A., and Nakicenovic, N.: Scenarios of long-term socio-economic
1003 and environmental development under climate stabilization, Technol. Forecast. Soc.
1004 Change, 74, 887-935, https://doi.org/10.1016/j.techfore.2006.05.026, 2007.
1005 Riahi, K., Krey, V., Rao, S., Chirkov, V., Fischer, G., Kolp, P., Kindermann, G.,
1006 Nakicenovic, N., and Rafai, P.: RCP8.5-exploring the consequence of high emission
1007 trajectories, Climatic Change, 109:33, https://doi.org/10.1007/s10584-011-0149-y,
1008 2011.
1009 Ramankutty, N., Evan, A. T., Monfreda, C., and Foley, J. A.: Farming the planet: 1.
1010 Geographic distribution of global agricultural lands in the year 2000, Glob.
1011 Biogeochem. Cyc., 22, GB1003, https://doi.org/10.1029/2007GB002952, 2008.
1012 Sadiq, M., Tai, A. P. K., Lombardozzi, D., and Val Martin, M.: Effects of ozone-
1013 vegetation coupling on surface ozone air quality via biogeochemical and

meteorological feedbacks, Atmos. Chem. Phys. 17, 3055-3066, https://doi.org/10.5194/acp-17-3055-2017, 2017.

Schnell, J. L., Prather, M. J., Josse, B., Naik, V., Horowitz, L. W., Zeng, G., Shindell, D. T., and Faluvegi, G.: Effect of climate change on surface ozone over North America, Europe, and East Asia, Geophys. Res. Lett., 43, 3509-3518, https://doi.org/10.1002/2016GL068060, 2016.

Squire, O. J., Archibald, A. T., Abraham, N. L., Beerling, D. J., Hewitt, C. N., Lathière, J., Pike, R. C., Telford, P. J., and Pyle, J. A.: Influence of future climate and cropland expansion on isoprene emissions and tropospheric ozone, Atmos. Chem. Phys., 14, 1011-1024, https://doi.org/10.5194/acp-14-1011-2014, 2014.

Shen, L., Mickley, L. J., and Gilleland, E.: Impact of increasing heat waves on US ozone episodes in the 2050s: Results from a multimodel analysis using extreme value theory, Geophys. Res. Lett., 43, 4017-4025, https://doi.org/10.1002/2016GL068432, 2016.

Swann, A. L. S., Fung, I. Y., and Chiang, J. C. H.: Mid-latitude afforestation shifts general circulation and tropical precipitation, Proc. Natl. Acad. Sci., USA, 109, 712-716, https://doi.org/10.1073/pnas.1116706108, 2012.

Tai, A. P. K., Mickley, L. J., Heald, C. L., and Wu, S.: Effect of CO2 inhibition on biogenic isoprene emission: Implications for air quality under 2000 to 2050 changes in climate, vegetation, and land use, Geophys. Res. Lett., 40, 3479-3483, https://doi.org/10.1002/grl.50650, 2013.

Tai, A. P. K., Val Martin, M. and Heald, C. L.: Threat to Future Global Food Security from Climate Change and Ozone Air Pollution, Nat. Clim. Change, 4, 817-821, https://doi.org/10.1038/nclimate2317, 2014.

Tai, A. P. K., and Val Martin, M.: Impacts of ozone air pollution and temperature extremes on crop yields: Spatial variability, adaptation and implications for future food security, Atmos. Environ., 169, 11-21, DOI10.1016/j.atmosenv.2017.09.002, 2017.

Taylor, K. E., Stouffer, R. J., and Meehl, G. A.: An overview of CMIP5 and the experiment design, Bull. Am. Meteorol. Soc., 93, 485-498, https://doi.org/10.1175/BAMS-D-11-00094.1, 2012.

Thomson, A. M., Calvin, K. V., Smith, S. J., Kyle, G. P., Volke, A., Patel, P., Delgado-Arias, S., and Bond-Lamberty, B.: RCP4.5: a pathway for stabilization of radiative forcing by 2100, Climatic Change, 109, 77-94, https://doi.org/10.1007/s10584-011-0151-4, 2011.

Thornton, J. A., Wooldridge, P. J., Cohen, R. C., Martinez, M., Harder, H., Brune, W. H., Williams, E. J., Roberts, J. M., Fehsenfeld, F. C., Hall, S. R., Shetter, R. E., Wert, B. P., and Fried, A.: Ozone production rates as a function of NOx abundances and HOx production rates in the Nashville urban plume, J. Geophys. Res., 107, 4146(D12), 4146, doi:10.1029/2001JD000932, 2002.

Tian, H., Ren, W., Tao, B., Sun, G., Chappelka, A., Wang, X., Pan, S., Yang, J., Liu, J., Felzer, B., Melillo, J., and Reilly, J.: Climate extremes and ozone pollution: a growing threat to China's food security, Ecosystem Health and Sustainability, 2, e01203, https://doi.org/10.1002/ehs2.1203, 2016.

Tilmes, S.: GEOS5 Global Atmosphere Forcing Data. Research Data Archive at the National Center for Atmospheric Research, Computational and Information Systems Laboratory, http://rda.ucar.edu/datasets/ds313.0/, 2016.

Unger, N.: Human land-use-driven reduction of forest volatiles cools global climate, Nat. Clim. Change, 4, 907-910, https://doi.org/10.1038/nclimate2347, 2014.

1063 Val Martin, M., Heald, C. L., and Arnold, S. R.: Coupling dry deposition to
1064 vegetation phenology in the Community Earth System Model: Implications for the
1065 simulation of surface O_3, Geophys. Res. Lett., 41, 2988-2996,
1066 https://doi.org/10.1002/2014GL059651, 2014.
1067 Val Martin, M., Heald, C. L., Lamarque, J.-F., Tilmes, S., Emmons, L. K., and
1068 Schichtel, B. A.: How emissions, climate, and land use change will impact mid-centry
1069 air quality over the United States: a focus on effects at national parks, Atmos. Chem.
1070 Phys., 15, 2805-2823, https://doi.org/10.5194/acp-15-2805-2015, 2015.
1071 van der Molen, M. K., van den Hurk, B. J. J. M., and Hazeleger, W.: A dampened
1072 land use change climate response towards the tropics, Clim. Dyn., 37, 2035-2043,
1073 https://doi.org/10.1007/s00382-011-1018-0, 2011.
1074 van Vuuren, D. P., den Elzen, M. G. J., Lucas, P. L., Eickhout, B., Strengers, B. J.,
1075 van Ruijven, B., Wonink, S., and van Houdt, R.: Stabilizing greenhouse gas
1076 concentrations at low levels: an assessment of reduction strategies and costs, Climatic
1077 Change, 81, 119-159, https://doi.org/10.1007/s10584-006-9172-9, 2007.
1078 van Vuuren, D. P., Edmonds, J., Kainuma, M., Riahi, K., Thomson, A., Hibbard, K.,
1079 Hurtt, G. C., Kram, T., Krey, V., Lamarque, J. F., Masui, T., Meinshausen, M.,
1080 Nakicenovic, N., Smith, S. J., and Rose, S. K.: The representative concentration
1081 pathways: an overview, Climatic Change, 109, 5-31, https://doi.org/10.1007/s10584-
1082 011-0148-z, 2011.
1083 Verbeke, T., Lathière, J., Szopa, S., and de Noblet-Ducoudré, N.: Impact of future
1084 land-cover changes on HNO_3 and O_3 surface dry deposition, Atmos. Chem. Phys., 15,
1085 13555-13568, https://doi.org/10.5194/acp-15-13555-2015, 2015.

von Kuhlmann, R., Lawrence, M. G., Poschl, U., and Crutzen, P. J.: Sensitivities in global scale modeling of isoprene, Atmos. Chem. Phys., 4, 1-17, https://doi.org/10.5194/acp-4-1-2004, 2004.

Wang, Y., Zhang, Y., Hao, J., and Luo, M.: Seasonal and spatial variability of surface ozone over China: contributions from background and domestic pollution, Atmos. Chem. Phys., 11, 3511-3525, https://doi.org/10.5194/acp-11-3511-2011, 2011.

Wang, Y., Shen, L., Wu, S., Mickley, L., He, J., and Hao, J.: Sensitivity of surface ozone over China to 2000-2050 global changes of climate and emissions, Atmos. Environ., 75, 374-382, https://doi.org/10.1016/j.atmosenv.2013.04.045, 2013.

Wesely, M.: Parameterization of surface resistances to gaseous dry deposition in regional-scale numerical models, Atmos. Environ., 23, 1293-1304, https://doi.org/10.1016/0004-6981(89)90153-4, 1989.

Wise, M., Calvin, K., Thomson, A., Clarke, L., Bond-Lamberty, B., Sands, R., Smith, S., J., Janetos, A., and Edmonds, J.: Implication of limiting CO2 concentrations for land use and energy, Science, 324, 1183-1186, DOI: 10.1126/science.1168475, 2009a.

Wise, M., Calvin, K., Thomson, A., Clarke, L., Sands, R., Smith, S. J., Janetos, A., and Edmonds, J.: The Implications of Limiting CO_2 Concentrations for Agriculture, Land-use Change Emissions, and Bioenergy, Technical Report, DOE Pacific Northwest National Laboratory, 2009b.

Wong, A. Y. H., Tai, A. P. K., and Ip, Y.-Y.: Attribution and statistical parameterization of the sensitivity of surface ozone to changes in leaf area index based on a chemical transport model, J. Geophys. Res. Atmos., 123, 1883-1898, https://doi.org/10.1002/2017JD027311, 2018.

World Health Organization: WHO Air quality guidelines for particulate matter, ozone, nitrogen dioxide and sulfur dioxide, Global update 2005, Summary of risk assessment, 2005. (http://apps.who.int/iris/bitstream/10665/69477/1/WHO_SDE_PHE_OEH_06.02_eng.pdf).

Wu, S., Mickley, L. J., Kaplan, J. O., and Jacob, D. J.: Impacts of changes in land use and land cover on atmospheric chemistry and air quality over the 21st century, Atmos. Chem. Phys., 12, 1597-1609, https://doi.org/10.5194/acp-12-1597-2012, 2012.

Xu, Z., Mahmood, R., Yang, Z.-L., Fu, C., and Su, H. Investigating diurnal and seasonal climatic response to land use and land cover change over monsoon Asia with the Community Earth System Model. J. Geophys. Res. Atmos., 120, 1137-1152. https://doi.org/10.1002/2014JD022479, 2015.

Xue, L., Wang, T., Louie, P. K. K., Luk, C. W. Y., Blake, D. R., and Xu, Z.: Increasing external effects negate local efforts to control ozone air pollution: A case study of Hong Kong and implications for other Chinese cities, Environ. Sci. Technol., 48, 10769-10775, https://doi.org/10.1021/es503278g, 2014.

Yienger, J. J., and Levy II H.: Empirical model of global soil-biogenic NO_x emissions, J. Geophys. Res. Atmos., 100, 11447-11464, https://doi.org/10.1029/95JD00370, 1995.

Yue, X. and Unger, N.: Ozone vegetation damage effects on gross primary productivity in the United States, Atmos. Chem. Phys., 14, 9137-9153, https://doi.org/10.5194/acp-14-9137-2014, 2014.

Zhang, Q., Yuan, B., Shao, M., Wang, X., Lu, S., Lu, K., Wang, M., Chen, L., Chang, C.-C., and Liu, S. C.: Variations of ground-level O_3 and its precursors in Beijing in

summertime between 2005 and 2011, Atmos. Chem. Phys., 14, 6089-6101, https://doi.org/10.5194/acp-14-6089-2014, 2014.

Zhou, D., Ding, A., Mao, H., Fu, C., Wang, T., Chan, L. Y., Ding, K., Zhang, Y., Liu, J., Lu, A., Hao, N.: Impacts of the East Asian monsoon on lower tropospheric ozone over coastal South China, Environ. Res. Lett., 8, 044011, doi:10.1088/1748-9326/8/4/044011, 2013.